New Developments and Applications of Thermal Field Theory[1]

by Markus H. Thoma[2,3]

Theory Division, CERN, CH-1211 Geneva 23, Switzerland

Abstract

The lecture provides an introduction to thermal field theory and its applications to the physics of the quark-gluon plasma, possibly created in relativistic heavy ion collisions. In particular the Hard Thermal Loop resummation technique, providing a consistent perturbative description of relativistic, high-temperature plasmas is introduced. Using this method interesting quantities of the quark-gluon plasma (damping rates, energy loss, photon and dilepton production) are discussed. Furthermore recent developments on non-equilibrium field theory, which are relevant for high-energy heavy ion physics, are presented.

Contents

[1] Lectures given at the Jyväskylä Summer School 2000

[2] Email: markus.thoma@cern.ch

[3] Heisenberg Fellow

1 Introduction and Motivation

The aim of relativistic heavy ion collision experiments is the discovery of a new state of matter, the so-called quark-gluon plasma (QGP). Quarks are substructure particles of hadrons. The observed hadron spectrum can be described by 6 different quark flavors (up, down, strange, charm, bottom, and top). Baryons contain 3 quarks, e.g. the proton 2 up and 1 down quarks. Meson consists of a quark and an antiquark, e.g. $\pi^+ \hat{=} u\,\bar{d}$.

The strong interaction between quarks is described within QCD, where the interaction is caused by the exchange of gauge bosons, the so-called gluons, analogously to photons in QED mediating the electromagnetic interaction. In contrast to QED quarks have three "charges" (and "anticharges") of the strong interaction, called color. As a consequence QCD is a non-abelian gauge theory based on the $SU(3)$ group. Also in contrast to QED the $SU(3)$ group leads to 8 gauge bosons, which can interact directly with themselves. The gluon self-interaction causes asymptotic freedom, i.e., quarks and gluons interact weakly at small distances or large momentum transfers. At large distances, however, the potential between partons (quarks and gluons) seems to increase linearly, which explains confinement, i.e., the absence of free quarks and gluons in nature. In this picture nucleons and other hadrons can be regarded as quark bags, containing besides the valence quarks also virtual quarks (sea quarks) and gluons, which force the partons to stay inside of the bag.

A nucleus can be pictured as a dense system of quark bags. If one increases the baryon density, e.g. by compressing the nucleus, or adds further hadrons, e.g. by increasing the temperature leading to thermal pion production, these bags will overlap. Then the quarks and gluons are not restricted to individual bags anymore but can move around in the entire system, which is now in the QGP phase. This deconfinement transition is expected to occur at a critical baryon density of the order of 10 times nuclear density ρ_0, where $\rho_0 = 0.125$ GeV/fm^3 $= 2.2 \times 10^{17}$ kg/m^3. The critical temperature is estimated by lattice calculations (see below) to be in the range of $T_c = 150 - 200$ MeV $= (1.8 - 2.4) \times 10^{12}$ K. These considerations give rise to the phase diagram shown in Fig.1. In nature the deconfinement phase transition occurred during the expansion of the early Universe about 2 microseconds after the Big Bang at zero baryon density (almost equal number of quarks and antiquarks). It might be realized also in the core of neutron stars at high baryon density. In the laboratory the fireball created in relativistic heavy ion collisions could be in the QGP phase for a short time period.

At this point let me make a few remarks:

1. The QGP is a relativistic plasma, i.e., the thermal velocity of the up-, down-quarks, and gluons is relativistic, since their masses are much smaller than the temperature of the plasma.

2. The QGP has the astonishing behaviour that it approaches the ideal gas limit for large densities and temperatures, because the parton interaction becomes weak due to asymptotic freedom.

3. Are there alternatives to the QGP at high temperature? Could it be that the deconfinement transition is never complete even at arbitrary high temperatures?

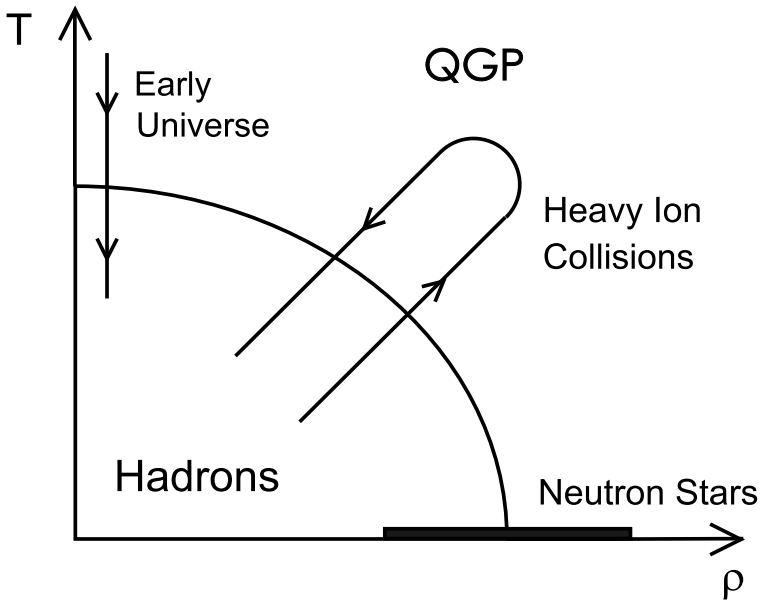

Fig.1

Maybe new non-perturbative configurations like QCD monopoles exist even in the high temperature limit? In order to answer this question the first step must be to identify the QGP state in relativistic heavy ion collisions.

There are two possible scenarios for producing a QGP fireball in relativistic heavy ion collisions. At relatively small center of mass energies, i.e. $\sqrt{s} \ll 100$ A·GeV, one expects that the Lorentz contracted nuclei stop each other in the collision and a hot, highly compressed fireball with a finite baryon or quark density (finite chemical potential), according to the surplus of quarks over anti-quarks from the nuclei, is created. At much higher energies, however, $\sqrt{s} \gtrsim 100$ A·GeV, there is not enough time for stopping and the nuclei penetrate each other transparently. However, the vacuum in the space-time volume between the nuclei after the collision is highly excited leading to a violent production of gluons and quark-antiquark pairs. Hence we expect the formation of a hot parton gas at zero baryon density (zero chemical potential). The both scenarios are sketched in Fig.2.

In the table below former, present, and future experiments with relativistic heavy ions are listed. Also a rough estimate for the maximum temperature reachable in these collisions is given.

Accelerator	Projectile-Target	$\sqrt{s}$ [A·GeV]	T_{max}[MeV]
AGS (BNL)	*Si-Au*, *Au-Au*	4-5	150
SPS (CERN)	*S-U*, *Pb-Pb*	17-20	190
RHIC (BNL)	*Au-Au*	200	230
LHC (CERN)	*Pb-Pb*	5500	260

How does a high energy nucleus-nucleus collision proceed in space and time? The space-time evolution of the fireball in the ultrarelativistic case, $\sqrt{s} \gtrsim 100$ A·GeV, is

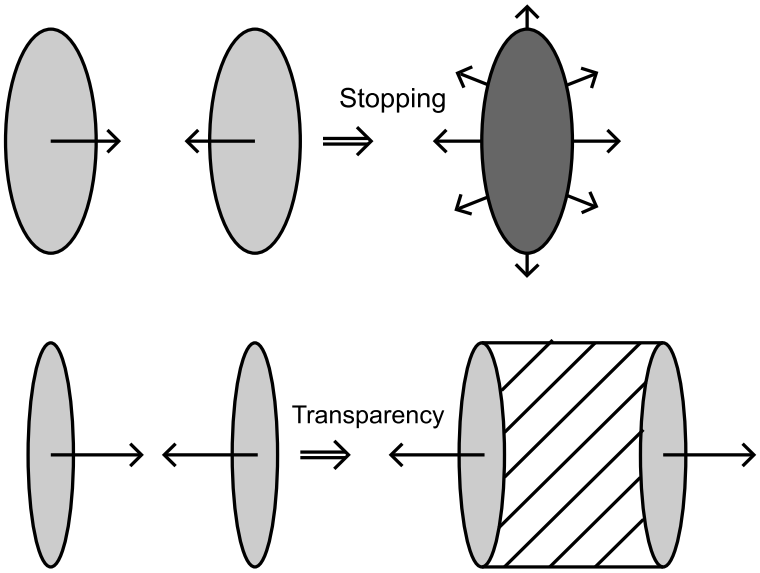

Fig.2

shown in Fig.3. The x-axis shows the beam direction and the y-axis the time, with $t = 0$ at the maximum overlap of the nuclei. The produced particles in this diagram lie only above the light-cone due to causality. The hyperbolas denote curves of constant proper time $\tau = \sqrt{t^2 - z^2}$. At the beginning the parton gas will be not in equilibrium. Only secondary collisions between the partons will lead to equilibration. Afterwards the temperature of the fireball will decrease in the course of its expansion until the critical temperature has been reached. Then the system will hadronize, maybe showing a substantial mixed phase, depending on the order of the phase transition. Finally the system will be so dilute that the interactions between the hadrons cease (freeze-out).

In order to speak of the QGP as a thermal system, we need a large volume and particle number, and a sufficient life time of the equilibrated system. The following rough estimates from simple models support the possibility of a QGP formation in heavy ion collisions: maximum volume (U-U) $\sim$ 3000 fm^3; parton number $\sim$ 10000; pre-equilibrium period $\sim$ 1 fm/c $= 3 \times 10^{-24}$ s; lifetime of QGP $\sim$ 5 - 10 fm/c.

The main problem is the identification of the QGP phase during the early stage of the fireball. Hadronic signatures (e.g. J/ψ-suppression or strangeness enhancement) are often strongly affected by final state interactions in the hadronic phase, while electromagnetic signals (photons, lepton pairs) are covered up by a huge background of hadronic decays.

In order to understand the properties of a QGP and to make unambiguous predictions about signatures for the QGP formation, we need a profound description of the QGP. For this purpose we have to use QCD at finite temperature and chemical potential. There are two different approaches.

1. Lattice QCD is a non-perturbative method for solving the QCD equations numerically on a 4-dimensional space-time lattice. In this way all temperatures from below to above the phase transition are accessible. Static quantities as the critical

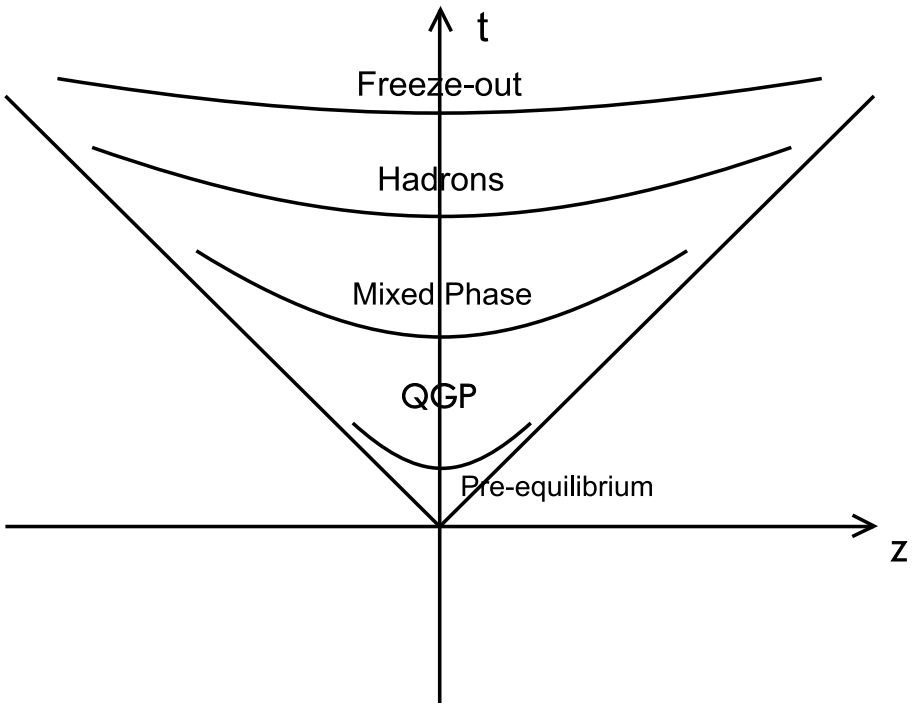

Fig.3

temperature, the order of the phase transition, or the equation of state of the QGP have been investigated successfully in this way. However, it is not possible (or at least very difficult) to address dynamical quantities, such as the most signatures for the QGP formation, a finite chemical potential, and non-equilibrium situations.

2. Perturbative QCD at finite temperature is based on the fact that the temperature dependent running coupling constant is small at high temperatures due to asymptotic freedom, $T \to \infty \Rightarrow \alpha_s(T) = g^2/4\pi \to 0$. At a typical temperature of $T = 250$ MeV we expect $\alpha_s = 0.3$ – 0.5. This suggest that perturbation theory could work at least qualitatively. It corresponds to an expansion in α_s, which can be performed conveniently by using Feynman diagrams as the ones in Fig.4 for elastic quark-quark scattering. In this way cross sections, life times, production and decay rates etc. can be calculated. The advantages compared to lattice calculations are, that one can compute static *and* dynamical quantities at $T > 0$ *and* $\mu > 0$ and that an extension to non-equilibrium is possible (see chapter 5). The drawbacks are that it is reliable only at high temperatures ($T \gg T_c$) and that one encounters infrared singularities, as we will discuss in the following in detail.

Finally let me note in this motivation of thermal field theory that there are more applications besides the QGP in relativistic heavy ion collisions, namely interactions of neutrinos and other particles in Supernovae plasmas, a possible quark matter core in neutron stars, the origin of the baryon asymmetry in the early Universe, and Bose condensates in condensed matter physics.

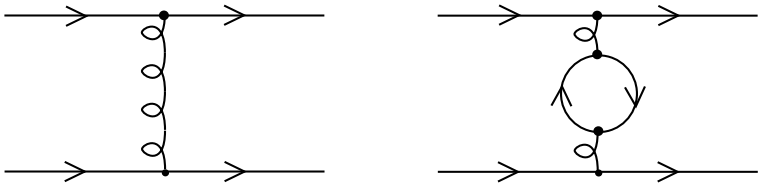

Fig.4

2 Introduction to Thermal Field Theory

2.1 Green functions at $T > 0$

The aim of this lecture is the introduction to thermal field theory (TFT) for allowing perturbative calculation of cross sections, life times, rates, etc. of particles in an equilibrated, relativistic medium. Thermal field theory is a combination of all three basic branches of modern physics, namely quantum mechanics, theory of relativity, and statistical physics. Therefore one could also call it relativistic quantum statistics.

Our aim is to derive Feynman diagrams and rules at $T > 0$ ($\mu \neq 0$). The most important quantity in perturbative field theory is the 2-point Green function or propagator. Therefore we have to ask first: How do propagators look like at $T > 0$? (In the non-relativistic case Green functions at finite temperature are discussed e.g. in *Fetter, Walecka, Quantum Theory of Many-Particle Systems.*) Here we want to discuss the scalar field theory first, which we will use in the following as a simple toy model to study the different techniques in TFT.

In order to set the notations and for comparing with the vacuum case, we repeat some basic facts about quantum field theory at zero temperature. The Feynman propagator is defined as

$$i\,\Delta_F(x-y) \equiv \langle 0|T\{\phi(x)\phi(y)\}|0\rangle, \tag{1}$$

where the scalar field can be expressed by the Fourier transform

$$\phi(x) = \int \frac{d^3k}{(2\pi)^{3/2}} \frac{1}{(2\omega_k)^{1/2}} \left[a(\mathbf{k})e^{-iK\cdot x} + a^\dagger(\mathbf{k})e^{iK\cdot x}\right]\Big|_{k_0=\omega_k}. \tag{2}$$

Here $x \equiv (x_0, \mathbf{x})$, $x_0 \equiv t$ using natural units $\hbar = c = k_B = 1$. We use the Minkowski metric, $x^2 = x_\mu x^\mu = g_{\mu\nu}x^\nu x^\mu = x_0^2 - \mathbf{x}^2$. Four momenta are denoted by $K \equiv (k_0, \mathbf{k})$, $k \equiv |\mathbf{k}|$ and the energy of the field is given by $\omega_k = \sqrt{k^2 + m^2}$. The time ordered product of two fields is defined as

$$T\{\phi(x)\phi(y)\} = \begin{cases} \phi(x)\phi(y) & x_0 > y_0 \\ \phi(y)\phi(x) & x_0 < y_0 \end{cases}.$$

The Fourier coefficients in (2) represent creation $a^\dagger(\mathbf{k})$ and destruction operators $a(\mathbf{k})$, which create or destroy a boson with momentum $\mathbf{k}$ in the state of the system. In particular the vacuum state is given by $a(\mathbf{k})|0\rangle = 0$ for all $\mathbf{k}$.

Using (1) and (2) the Feynman propagator can be written as

$$\Delta_F(x-y) = \int \frac{d^4K}{(2\pi)^4} \frac{e^{-iK\cdot(x-y)}}{K^2 - m^2 + i\epsilon}. \tag{3}$$

From this expression we can derive the Feynman rule for the propagator in momentum space. Δ_F describes the free propagation of a free scalar particle from y to x for $x_0 > y_0$ (creation at y, destruction at x) and from x to y for $x_0 < y_0$. Integrating over k_0 in the complex k_0-plane we find in the case $x_0 > y_0$

$$\Delta_F(x-y) = -i \int \frac{d^3k}{(2\pi)^3} \frac{1}{2\omega_k} e^{-iK\cdot(x-y)}\Big|_{k_0=\omega_k}. \tag{4}$$

Now let us turn to $T > 0$. Vacuum expectation values have now to be replaced by quantum statistic expectation values, i.e.

$$\langle A \rangle \equiv \mathrm{Tr}\,(\rho A), \tag{5}$$

where A is an arbitrary quantum operator and ρ the density operator or matrix. Choosing the canonical ensemble it is given by

$$\rho = \frac{1}{Z}\, e^{-\beta H}, \tag{6}$$

where $\beta \equiv 1/T$, H is the Hamiltonian of the system with the eigenvalues and eigenstates $H|n\rangle = E_n|n\rangle$. (For $\mu \neq 0$ H is replaced by $H - \mu N$ with the number operator N.) The partition function is $Z = \mathrm{Tr}\,(e^{-\beta H})$. Then we can write

$$\langle A \rangle = \frac{1}{Z}\,\mathrm{Tr}\,(Ae^{-\beta H}) = \frac{1}{Z}\,\sum_n \langle n|A|n\rangle\, e^{-\beta E_n}, \tag{7}$$

where the sum goes over all thermally exited states weighted with the Boltzmann factor $|n\rangle$ and $\exp(-\beta E_n)$.

(It is possible to formulate the Boltzmann factor in a Lorentz invariant way by introducing the four velocity u_μ: $\exp\,(-\beta u_\mu P^\mu)$ with $p_0 = E$. In the following we will consider only the Lorentz frame of heat bath: $u_\mu = (1, 0, 0, 0)$.)

Now we will apply (7) to the scalar propagator, yielding

$$i\,\Delta_F^{T>0}(x-y) = \frac{1}{Z}\,\sum_n \langle n|T\{\phi(x)\phi(y)\}|n\rangle\, e^{-\beta E_n}\ . \tag{8}$$

Using (2) in (8) for $x_0 > y_0$ we obtain

$$\begin{aligned} i\,\Delta_F^{T>0}(x-y) &= \frac{1}{Z}\int \frac{d^3k}{(2\pi)^{3/2}}\frac{d^3k'}{(2\pi)^{3/2}}\frac{1}{(2\omega_k)^{1/2}}\frac{1}{(2\omega'_k)^{1/2}}\sum_n e^{-\beta E_n} \\ &\langle n|[a(\mathbf{k})e^{-iK\cdot x} + a^\dagger(\mathbf{k})e^{iK\cdot x}]\,[a(\mathbf{k}')e^{-iK'\cdot y} + a^\dagger(\mathbf{k}')e^{iK'\cdot y}]|n\rangle. \end{aligned} \tag{9}$$

The multi-boson states are given by acting repeatedly with the creation operator on the vacuum state according to

$$|n\rangle = |n_1(\mathbf{k}_1), n_2(\mathbf{k}_2), ...\rangle = \prod_i \frac{[a^\dagger(\mathbf{k}_i)]^{n_i(\mathbf{k}_i)}}{\sqrt{n_i(\mathbf{k}_i)!}}\,|0\rangle. \tag{10}$$

The states $|n\rangle$ are orthonormalized. In order to evaluate (9) we need

$$\begin{aligned} a(\mathbf{k}_i)|n\rangle &= \sqrt{n(\mathbf{k}_i)}\,|n_1(\mathbf{k}_1), n_2(\mathbf{k}_2), ..., n_i(\mathbf{k}_i) - 1, ...\rangle, \\ a^\dagger(\mathbf{k}_i)|n\rangle &= \sqrt{n(\mathbf{k}_i) + 1}\,|n_1(\mathbf{k}_1), n_2(\mathbf{k}_2), ..., n_i(\mathbf{k}_i) + 1, ...\rangle, \end{aligned} \tag{11}$$

which leads to

$$\begin{aligned} i\,\Delta_F^{T>0}(x-y) &= \frac{1}{Z}\int \frac{d^3k}{(2\pi)^{3/2}}\frac{d^3k'}{(2\pi)^{3/2}}\frac{1}{(2\omega_k)^{1/2}}\frac{1}{(2\omega'_k)^{1/2}}\sum_n e^{-\beta E_n} \\ &\{[n(\mathbf{k})+1]\delta^3(\mathbf{k}-\mathbf{k}')e^{-iK\cdot x + iK'\cdot y} + n(\mathbf{k})\delta^3(\mathbf{k}-\mathbf{k}')e^{iK\cdot x - iK'\cdot y}\} \\ &= \frac{1}{Z}\int \frac{d^3k}{(2\pi)^3}\frac{1}{2\omega_k}\sum_n e^{-\beta E_n}\{[n(\mathbf{k})+1]e^{-iK\cdot(x-y)} + n(\mathbf{k})e^{iK\cdot(x-y)}\}\Big|_{k_0=\omega_k}. \end{aligned} \tag{12}$$

Now we use

$$\frac{1}{Z}\sum_n n(\mathbf{k})e^{-\beta E_n} = \frac{1}{\exp(\beta\omega_k)-1} \equiv n_B(\omega_k) \tag{13}$$

where $E_n = \sum_{\mathbf{k}} \omega_k n(\mathbf{k})$ (see e.g. *Reif, Fundamentals of Statistical and Thermal Physics*) and $n_B(\omega_k)$ is the Bose-Einstein distribution. (In the case of fermions, we have according to the Pauli exclusion principle $n(\mathbf{k})\epsilon\{0,1\}$, from which the Fermi-Dirac distribution $n_F(\omega_k) = 1/[\exp(\beta(\omega_k-\mu))+1]$ follows. Owing to particle number conservation, e.g. charge or baryon number conservation, the average number of particles is fixed, which is taken into account by introducing the chemical potential μ.) Combining (12) and (13) we find

$$i\,\Delta_F^{T>0}(x-y) = \int \frac{d^3k}{(2\pi)^3}\,\frac{1}{2\omega_k}\,\left\{[1+n_B(\omega_k)]\,e^{-iK(x-y)} + n_B(\omega_k)\,e^{iK(x-y)}\right\}. \tag{14}$$

Indeed for $T=0$, i.e. $n_B = 0$, we recover the vacuum result (4).

The physical interpretation of this expression is the following: As at zero temperature the finite temperature propagator describes the propagation of a scalar particle from y to x ($x_0 > y_0$). However, besides spontaneous creation at y there is also induced creation ($\sim n_B$) and absorption ($\sim n_B$) at x due to the presence of the thermal particles in the heat bath.

Next we want to give a 4-dimensional K-integral representation of $\Delta_F^{T>0}$ from which we can derive Feynman rules in momentum space.

2.2 Imaginary Time Formalism (ITF)

We start with the following statement: Going to imaginary times t with $0 \le \tau \equiv it < \beta$ and summing over discrete energies $k_0 = 2\pi i n T$ (Matsubara frequencies) instead of integrating, i.e.,

$$\int \frac{dk_0}{2\pi} \to iT \sum_{n=-\infty}^{\infty},$$

the propagator (14) can be written as

$$i\,\Delta_F^{T>0}(x) = iT\,\sum_n \int \frac{d^3k}{(2\pi)^3}\,\frac{i}{K^2-m^2}\,e^{-iK\cdot x}. \tag{15}$$

Proof: (15) can be written as

$$i\,\Delta_F^{T>0}(x) = -T\,\int \frac{d^3k}{(2\pi)^3}\,\sum_n \frac{1}{k_0^2-\omega_k^2}\,e^{-k_0\cdot\tau}\,e^{i\mathbf{k}\cdot\mathbf{x}}.$$

Now we use the formula

$$\begin{aligned} T\sum_{n=-\infty}^{\infty} f(k_0 = 2\pi i n T) &= \frac{1}{2\pi i}\int_{-i\infty}^{i\infty} dk_0 \frac{1}{2}\,[f(k_0)+f(-k_0)] \\ &+ \frac{1}{2\pi i}\int_{-i\infty+\epsilon}^{i\infty+\epsilon} dk_0\,[f(k_0)+f(-k_0)]\,n_B(k_0), \end{aligned}$$

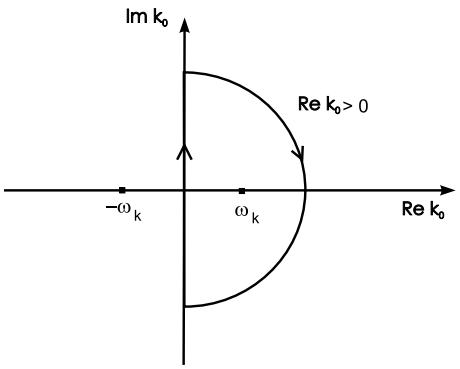

Fig.5

which holds if $f(k_0)$ has no poles on the imaginary axis (see problem #2).

Choosing

$$f(k_0) = \frac{-1}{k_0^2 - \omega_k^2}\, e^{-k_0\tau}$$

we get

$$-T \sum_{n=-\infty}^{\infty} \frac{1}{k_0^2 - \omega_k^2}\, e^{-k_0\cdot\tau} = I_1 + I_2 + I_3 + I_4,$$

with

$$\begin{aligned} I_1 &= -\frac{1}{2\pi i}\,\frac{1}{2}\int_{-i\infty}^{i\infty} dk_0\, \frac{e^{-k_0\tau}}{k_0^2 - \omega_k^2} \\ &= \frac{1}{2}\,\mathrm{Res}\left[\frac{e^{-k_0\tau}}{k_0^2 - \omega_k^2}\right]_{k_0=\omega_k} \\ &= \frac{1}{2}\,\frac{e^{-\omega_k\tau}}{2\omega_k}, \end{aligned}$$

where we have closed the contour in the half plane $\mathrm{Re}\, k_0 > 0$ (see Fig.5). Analogously, closing the contour for $\mathrm{Re}\, k_0 < 0$ we find $I_2 = I_1$.

Furthermore we have

$$\begin{aligned} I_3 &= -\frac{1}{2\pi i}\int_{-i\infty+\epsilon}^{i\infty+\epsilon} dk_0\, \frac{1}{k_0^2 - \omega_k^2}\frac{e^{-k_0\tau}}{e^{\beta k_0} - 1} \\ &= n_B(\omega_k)\,\frac{e^{-\omega_k\tau}}{2\omega_k}, \end{aligned}$$

where we have used the contour shown in Fig.6. For I_4 we have to use the same contour as in Fig.6, since $\beta > \tau$, yielding

$$I_4 = n_B(\omega_k)\,\frac{e^{+\omega_k\tau}}{2\omega_k}.$$

Combining these expressions we find

$$\begin{aligned} i\,\Delta_F^{T>0}(x) &= \int \frac{d^3k}{(2\pi)^3}\, e^{i\mathbf{k}\cdot\mathbf{x}}\,\left[\frac{e^{-\omega_k\tau}}{2\omega_k} + \frac{n_B(\omega_k)}{2\omega_k}\,\left(e^{-\omega_k\tau} + e^{\omega_k\tau}\right)\right] \\ &= \int \frac{d^3k}{(2\pi)^3}\,\frac{1}{2\omega_k}\,\left\{[1 + n_B(\omega_k)]\, e^{-i\omega_k t}\, e^{i\mathbf{k}\cdot\mathbf{x}} + n_B(\omega_k)\, e^{i\omega_k t}\, e^{i\mathbf{k}\cdot\mathbf{x}}\right\}. \end{aligned}$$

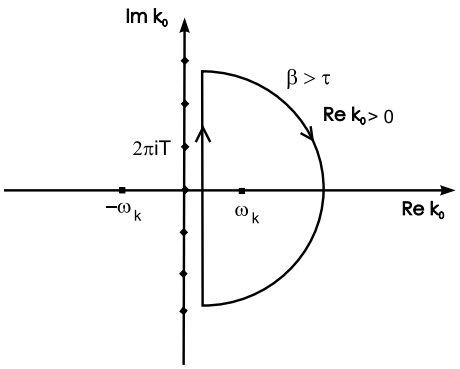

Fig.6

Replacing $\mathbf{k}$ by $-\mathbf{k}$ in the second part of the last expression we recover (14). □

Another motivation for introducing an imaginary time is the following: for $\tau = it \to \beta$ the Boltzmann factor $\exp(-\beta H)$ assumes the form of the time evolution operator $\exp(-iHt)$. As a consequence thermal propagators (more general, all Green functions) become periodic with β, since

$$\begin{aligned}
&\Delta_F^{T>0}(x-y) = \Delta_F^{T>0}(\mathbf{x},\mathbf{y},\tau,0) \qquad (\tau_x = \tau, \tau_y = 0)\\
&= \frac{1}{Z}\ \mathrm{Tr}\ \left[e^{-\beta H}\ T\{\phi(\mathbf{x},\tau)\phi(\mathbf{y},0)\}\right] \qquad (\beta > \tau > 0)\\
&= \frac{1}{Z}\ \mathrm{Tr}\ \left[e^{-\beta H}\ \phi(\mathbf{x},\tau)\ \phi(\mathbf{y},0)\right]\\
&= \frac{1}{Z}\ \mathrm{Tr}\ \left[\phi(\mathbf{y},0)\ e^{-\beta H}\ \phi(\mathbf{x},\tau)\right]\\
&= \frac{1}{Z}\ \mathrm{Tr}\ \left[e^{-\beta H}\ e^{\beta H}\ \phi(\mathbf{y},0)\ e^{-\beta H}\ \phi(\mathbf{x},\tau)\right]\\
&= \frac{1}{Z}\ \mathrm{Tr}\ \left[e^{-\beta H}\ \phi(\mathbf{y},\beta)\ \phi(\mathbf{x},\tau)\right]\\
&= \frac{1}{Z}\ \mathrm{Tr}\ \left[e^{-\beta H}\ T\{\phi(\mathbf{x},\tau)\phi(\mathbf{y},\beta)\}\right]\\
&= \Delta_F^{T>0}(\mathbf{x},\mathbf{y},\tau,\beta).
\end{aligned}$$

In general

$$\Delta_F^{T>0}(\tau) = \Delta_F^{T>0}(\tau + n\beta) \qquad n \text{ integer} \tag{16}$$

holds. This has two consequences

1. The time τ is restricted to the interval $[0,\beta[$, known as Kubo-Martin-Schwinger- or KMS-condition.

2. The Fourier integral over k_0 at $T = 0$ goes over to a Fourier series over the Matsubara frequencies $k_0 = 2\pi i n T$.

(For fermions we have $S_F^{T>0}(\tau) = (-1)^n\, S_F^{T>0}(\tau + n\beta)$ due to a minus sign in the definition of time ordering corresponding to anti-commuting fields, from which we get $k_0 = (2n+1)i\pi T$.)

The Feynman rules in the ITF for example for the ϕ^4-theory now read:

1. The propagator is given by $i\,\Delta_F^{T>0}(K) = i/(K^2 - m^2)$ with $k_0 = 2\pi i n T$.

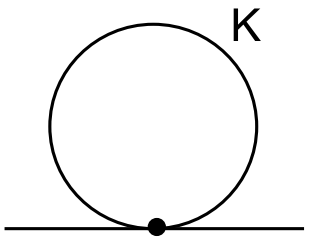

Fig.7

2. In loop integrals we have to make the replacement $\int d^4K/(2\pi)^4 \to iT\sum_{k_0}\int d^3k/(2\pi)^3$.

3. The vertex reads as in vacuum $-i\,4!\,g^2$. (In order to compare with gauge theories we denote the coupling constant as g^2.)

4. Symmetry factors, e.g. 1/2 for tadpole, are the same as in vacuum.

As the simplest example for a loop diagram we consider the tadpole of the ϕ^4-theory shown in Fig.7. According to the above Feynman rules it is given by

$$\begin{aligned}\Pi &= \frac{i}{2}\,(-i\,4!\,g^2)\,iT\sum_{k_0}\int\frac{d^3k}{(2\pi)^3}\,i\,\frac{1}{K^2-m^2}\\ &= -12\,g^2\,T\int\frac{d^3k}{(2\pi)^3}\sum_{n=-\infty}^{\infty}\frac{1}{(2\pi inT)^2-\omega_k^2}\\ &= 12\,g^2\,T\,\frac{1}{(2\pi T)^2}\int\frac{d^3k}{(2\pi)^3}\sum_{n=-\infty}^{\infty}\frac{1}{n^2+\Omega^2}\end{aligned}$$

with $\Omega\equiv\omega_k/(2\pi T)$. Using (see *Gradshteyn, Ryzhik, Tables of Integrals*)

$$\coth(\pi\Omega)=\frac{1}{\pi\Omega}+\frac{2\Omega}{\pi}\sum_{n=1}^{\infty}\frac{1}{n^2+\Omega^2}$$

we obtain

$$\begin{aligned}&\sum_{n=-\infty}^{\infty}\frac{1}{n^2+\Omega^2}=2\sum_{n=1}^{\infty}\frac{1}{n^2+\Omega^2}+\frac{1}{\Omega^2}=\frac{\pi}{\Omega}\,\coth(\pi\Omega)\\ &=\frac{\pi}{\Omega}\,\frac{e^{\pi\Omega}+e^{-\pi\Omega}}{e^{\pi\Omega}-e^{-\pi\Omega}}=\frac{\pi}{\Omega}\,\frac{e^{2\pi\Omega}+1}{e^{2\pi\Omega}-1}\\ &=\frac{\pi}{\Omega}\,\left(1+\frac{2}{e^{2\pi\Omega}-1}\right)=\frac{2\pi^2T}{\omega_k}\,[1+2n_B(\omega_k)]\end{aligned}$$

leading to

$$\Pi=6\,g^2\int\frac{d^3k}{(2\pi)^3}\,\frac{1}{\omega_k}\,[1+2n_B(\omega_k)]. \tag{17}$$

Note that only the vacuum part ($n_B=0$) is ultraviolet divergent, since the distribution functions falls off exponentially for large momenta. Hence we can use the same renormalization as at $T=0$. Using dimensional regularization the tadpole at $T=0$ vanishes, resulting in

$$\Pi=12\,g^2\,\frac{4\pi}{(2\pi)^3}\int_0^{\infty}dk\,\frac{k^2}{\omega_k}\,n_B(\omega_k).$$

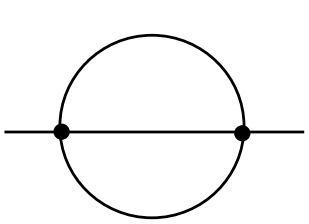

Fig.8

An analytic expression for this integral is only possible for $m = 0$, for which we get

$$\Pi = \frac{6}{\pi^2}\, g^2 \int_0^\infty dk\, \frac{k}{e^{k/T}-1} \stackrel{x\equiv k/T}{=} \frac{6}{\pi^2}\, g^2\, T^2 \int_0^\infty dx\, \frac{x}{e^x-1}.$$

Using

$$\int_0^\infty dx\, \frac{x^{n-1}}{e^x-1} = (n-1)!\,\zeta(n), \qquad\qquad \zeta(2) = \frac{\pi^2}{6}$$

we end up with the simple result

$$\Pi = g^2 T^2. \tag{18}$$

The problem is now that for diagrams with more than one propagator, e.g. the one shown in Fig.8, the summation over k_0 becomes difficult. A convenient way out of this problem is the so-called Saclay method which is a mixed representation performing the Fourier transformation in time only. (In the following we use $\Delta \equiv \Delta_F^{T>0}$.) This leads to

$$\Delta(\tau, \omega_k) = -T \sum_{k_0} e^{-k_0\tau}\, \Delta(K), \tag{19}$$

where the Fourier coefficients are given as

$$\Delta(K) = -\int_0^\beta d\tau\, e^{k_0\tau}\, \Delta(\tau, \omega_k). \tag{20}$$

Following the proof of (15) we can perform the sum (19),

$$\Delta(\tau, \omega_k) = \frac{1}{2\omega_k} \left\{ [1 + n_B(\omega_k)]\, e^{-\omega_k\tau} + n_B(\omega_k)\, e^{\omega_k\tau} \right\}.$$

Now the Matsubara frequency k_0, over which we have to sum, appears in the propagator (20) only in the exponent, which makes the summation simple at the expense of introducing another integral over τ. For example for the tadpole we get now

$$\begin{aligned} \Pi &= \frac{i}{2}\,(-i\,4!\,g^2)\, iT \sum_{k_0} \int \frac{d^3k}{(2\pi)^3}\, i\,(-1) \int_0^\beta d\tau\, e^{k_0\tau}\, \Delta(\tau, \omega_k) \\ &= 12\, g^2 \int \frac{d^3k}{(2\pi)^3} \int_0^\beta d\tau \Delta(\tau, \omega_k)\, T \sum_{n=-\infty}^{\infty} e^{k_0\tau}. \end{aligned}$$

The sum over k_0 reduces to a δ-function

$$T \sum_{n=-\infty}^{\infty} e^{k_0(\tau-\tau')} = T \sum_n e^{2\pi i n T(\tau-\tau')} = T\delta(T(\tau-\tau')) = \delta(\tau-\tau').$$

This formula makes the Saclay method very convenient in the case of two or more propagators. In the case of the tadpole it yields

$$\begin{aligned}\Pi &= 12\,g^2 \int \frac{d^3k}{(2\pi)^3}\Delta(0,\omega_k) \\ &= 6\,g^2 \int \frac{d^3k}{(2\pi)^3}\,\frac{1}{\omega_k}\,[1+2n_B(\omega_k)],\end{aligned}$$

which is identical to our result (17).

2.3 Real Time Formalism (RTF)

Here we do not aim at a formal derivation, but will present only a motivation and plausibility arguments. For a more detailed derivation the interested reader is referred e.g. to Ref.[2].

The starting point is again our basic equation (14) for the propagator,

$$i\,\Delta(x-y) = \int \frac{d^3k}{(2\pi)^3}\,\frac{1}{2\omega_k}\,\left\{[1+n_B(\omega_k)]\,e^{-iK(x-y)} + n_B(\omega_k)\,e^{iK(x-y)}\right\}\Big|_{k_0=\omega_k}.$$

Instead of introducing Matsubara frequencies we will give an alternative expression for writing (14) as a 4-dimensional integral, namely

$$i\,\Delta(x-y) = \int \frac{d^4K}{(2\pi)^4}\,\left[\frac{i}{K^2-m^2+i\epsilon} + 2\pi\,n_B(|k_0|)\,\delta(K^2-m^2)\right]\,e^{-iK(x-y)}. \quad (21)$$

The complex k_0-integration over the first term gives the $T=0$ term (4), i.e., the first term of (14) following from setting $n_B = 0$. The second term gives

$$\begin{aligned}&\int \frac{d^4K}{(2\pi)^4}\,2\pi\,n_B(|k_0|)\,\delta(K^2-m^2)\,e^{-iK(x-y)} \\ &= \int \frac{d^3k}{(2\pi)^3}\,dk_0\,n_B(|k_0|)\,\frac{1}{2\omega_k}\,[\delta(k_0-\omega_k)+\delta(k_0+\omega_k)]\,e^{-ik_0(x_0-y_0)}\,e^{i\mathbf{k}\cdot(\mathbf{x}-\mathbf{y})} \\ &= \int \frac{d^3k}{(2\pi)^3}\,\frac{n_B(\omega_k)}{2\omega_k}\,\left[e^{-i\omega_k(x_0-y_0)} + e^{i\omega_k(x_0-y_0)}\right]\,e^{i\mathbf{k}\cdot(\mathbf{x}-\mathbf{y})} \\ &= \int \frac{d^3k}{(2\pi)^3}\,\frac{1}{2\omega_k}\,\left[n_B(\omega_k)\,e^{-iK(x-y)} + n_B(\omega_k)\,e^{iK(x-y)}\right]\Big|_{k_0=\omega_k}, \end{aligned} \quad (22)$$

which proves the equivalence of (21) and (14).

The advantages of this representation are the following.

1. There is no Matsubara sum, but an integration over k_0 as at $T=0$.

2. We do not need an imaginary time, which is restricted to finite temperatures and cannot be generalized to non-equilibrium. Actually, as we will see in chapter 5, the RTF can be used as a starting point for non-equilibrium field theory.

3. The distribution functions appear from the beginning. Hence the $T=0$ and $T>0$ contributions are disentangled.

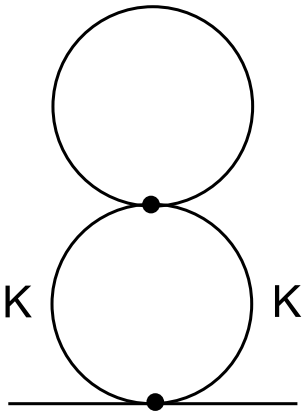

Fig.9

The Feynman rule in momentum space in the RTF for the scalar propagator reads now:

$$\frac{i}{K^2 - m^2 + i\epsilon} + 2\pi\, n_B(|k_0|)\, \delta(K^2 - m^2). \tag{23}$$

Otherwise we have the same rules as at $T = 0$.

The fermion propagator is given by

$$S(P) = (\not{P} + M)\, \left[\frac{i}{P^2 - M^2 + i\epsilon} - 2\pi\, n_F(|p_0|)\, \delta(P^2 - M^2)\right]. \tag{24}$$

Again we will consider the tadpole in ϕ^4-theory as an example. In the RTF it is given as

$$\begin{aligned}
\Pi &= \frac{i}{2}\,(-i\,4!\,g^2) \int \frac{d^4K}{(2\pi)^4}\, i\,\Delta(K) \\
&= 12\,g^2 \int \frac{d^4K}{(2\pi)^4}\, \left[\frac{i}{K^2 - m^2 + i\epsilon} + 2\pi\, n_B(|k_0|)\, \delta(K^2 - m^2)\right] \\
&= 12\,g^2 \int \frac{d^3k}{(2\pi)^3}\, dk_0\, n_B(|k_0|)\, \frac{1}{2\omega_k}\, [\delta(k_0 - \omega_k) + \delta(k_0 + \omega_k)] \\
&= 12\,g^2 \int \frac{d^3k}{(2\pi)^3}\, \frac{n_B(\omega_k)}{\omega_k},
\end{aligned}$$

where we have neglected the vacuum part, which vanishes after renormalization, again. This result coincides with the one, (17), found in the ITF.

Unfortunately there is a serious problem with the naive RTF, presented above. Singularities, so-called pinch singularities, coming from δ-functions are possible in diagrams with two or more propagators, as e.g. in Fig.9. The lower loop in this diagram is proportional to $\int d^4K \Delta^2(K) \sim \int d^4K\, [\delta(K^2 - m^2)]^2 \sim \delta(0) = \infty$.

A possible solution of this problem is the so-called "doubling of degrees of freedom". According to the KMS-condition the time of the fields goes from $t = 0$ to $t = -i\beta$. This contour can be deformed in order to include the real time axis by going first from $t = 0$ to $t = \infty$ above the real time axis and then back to $t = -i\beta$

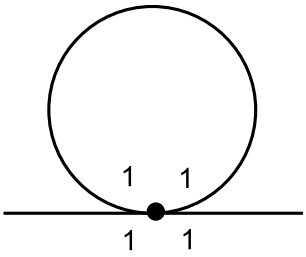

Fig.10

below the real time axis. This deformation corresponds to two different kind of fields, one existing above and one below the real time axis. Then the propagator, which contains two fields, is given by a 2×2 matrix (for details see e.g. Ref.[2])

$$\Delta(K) = \begin{pmatrix} \frac{1}{K^2-m^2+i\epsilon} & 0 \\ 0 & \frac{-1}{K^2-m^2-i\epsilon} \end{pmatrix} - 2\pi i\, \delta(K^2-m^2) \begin{pmatrix} n_B(k_0) & \theta(-k_0)+n_B(k_0) \\ \theta(k_0)+n_B(k_0) & n_B(k_0) \end{pmatrix}, \tag{25}$$

where we have used here and in the following $n_B(k_0) \equiv n_B(|k_0|)$.

The Feynman rules for the propagator read now $i\,\Delta_{ij}(K)$ with $i,j\epsilon\{1,2\}$. The vertex is given by $i\,(-1)^j\,g^2\,4!$. Fields from above and below the real time axis are not mixed at a vertex and the vertex of the "type-2-fields" has an additional minus sign coming from the anti-time ordering of the fields below the real time axis.

Again we consider the tadpole diagram as example. Also self energies are now given by matrices. The Π_{11} component, given by Fig.10, reads

$$\Pi_{11} = \frac{i}{2}\, i\,(-1)\, g^2\, 4! \int \frac{d^4K}{(2\pi)^4}\, 2\pi\, n_B(k_0)\, \delta(K^2-m^2),$$

which agrees with (17). The components $\Pi_{12} = \Pi_{21} = 0$, since all legs of the vertex must have the same index. The component $\Pi_{22} = -\Pi_{11}$ because of the minus sign from the "type-2-field" vertex.

It is important to note that the individual components of the propagator are not independent:

$$\begin{aligned}
&\Delta_{11} - \Delta_{12} - \Delta_{21} + \Delta_{22} \\
&= \frac{1}{K^2-m^2+i\epsilon} - 2\pi i\,\delta(K^2-m^2)\, n_B(k_0) + 2\pi i\,\delta(K^2-m^2)\,[\theta(-k_0)+n_B(k_0)] \\
&+2\pi i\,\delta(K^2-m^2)\,[\theta(k_0)+n_B(k_0)] - \frac{1}{K^2-m^2-i\epsilon} - 2\pi i\,\delta(K^2-m^2)\, n_B(k_0) \\
&= \frac{1}{K^2-m^2+i\epsilon} - \frac{1}{K^2-m^2-i\epsilon} + 2\pi i\,\delta(K^2-m^2) \\
&= \frac{-2i\epsilon}{(K^2-m^2)^2+\epsilon^2} + 2\pi i\,\delta(K^2-m^2) \\
&= 2i\,\mathrm{Im}\,\frac{1}{K^2-m^2+i\epsilon} + 2\pi i\,\delta(K^2-m^2) = 0,
\end{aligned} \tag{26}$$

where we have used for the last step the important relation

$$\delta(K^2-m^2) = -\frac{1}{\pi}\,\mathrm{Im}\,\frac{1}{K^2-m^2+i\epsilon}. \tag{27}$$

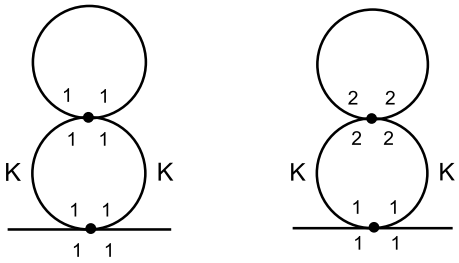

Fig.11

Note that in contrast to ITF factors $i\epsilon$ are important in RTF.

Now we consider the dangerous 2-loop diagrams, for which there are 2 contributions to Π_{11} as shown in Fig.11. The integral for the lower loop contains $\Delta_{11}(K)\Delta_{11}(K) - \Delta_{12}(K)\Delta_{21}(K)$. (Note the minus sign from the "type-2-field" vertex, which implies that the rules of matrix multiplication do not hold.) Explicitly this expression can be written as

$$
\begin{aligned}
&\left[\frac{1}{K^2-m^2+i\epsilon} - 2\pi i\,\delta(K^2-m^2)\,n_B(k_0)\right]^2 - (-2\pi i)\,\delta(K^2-m^2)\,[\theta(-k_0)+n_B(k_0)] \\
&\times(-2\pi i)\,\delta(K^2-m^2)\,[\theta(k_0)+n_B(k_0)] \\
&= \left(\frac{1}{K^2-m^2+i\epsilon}\right)^2 - \frac{1}{K^2-m^2+i\epsilon}\,4\pi i\,\delta(K^2-m^2)\,n_B(k_0) - 4\pi^2\,\delta^2(K^2-m^2)\,n_B^2(k_0) \\
&+4\pi^2\,\delta^2(K^2-m^2)[n_B(k_0)+n_B^2(k_0)] \\
&\overset{(27)}{=} \left(\frac{1}{K^2-m^2+i\epsilon}\right)^2 - \frac{1}{K^2-m^2+i\epsilon}\,4\pi i\,\delta(K^2-m^2)\,n_B(k_0) \\
&-\frac{1}{2\pi i}\,\left(\frac{1}{K^2-m^2+i\epsilon} - \frac{1}{K^2-m^2-i\epsilon}\right)\,4\pi^2\,\delta(K^2-m^2)\,n_B(k_0) \\
&= \left(\frac{1}{K^2-m^2+i\epsilon}\right)^2 - \left(\frac{1}{K^2-m^2+i\epsilon} + \frac{1}{K^2-m^2-i\epsilon}\right)\,2\pi i\,\delta(K^2-m^2)\,n_B(k_0) \\
&\overset{(27)}{=} {\Delta_0}^2(K) + n_B(k_0)\,[{\Delta_0}^2(K) - \Delta_0^{*2}(K)],
\end{aligned}
$$

where $\Delta_0 = 1/(K^2-m^2+i\epsilon)$. One observes that pinch singularities coming from products of δ-functions are absent due to a cancellation between the to diagrams in Fig.11. Similar arguments hold for higher order diagrams.

Now we will introduce a very convenient representation of the RTF, the *Keldysh representation*. It is constructed from linear combinations of the components of the RTF Green functions. The new components of the propagator are defined as

$$
\begin{aligned}
&\text{Retarded propagator: } \Delta_R \equiv \Delta_{11} - \Delta_{12}, \\
&\text{Advanced propagator: } \Delta_A \equiv \Delta_{11} - \Delta_{21}, \\
&\text{Symmetric propagator: } \Delta_S \equiv \Delta_{11} + \Delta_{22}.
\end{aligned}
\tag{28}
$$

The component Δ_S is often denoted as Δ_F in the literature. There are only 3 components, which is sufficient because of (26).

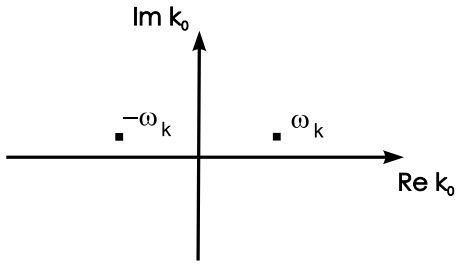

Fig.12

The inverse relations read

$$\begin{aligned}
\Delta_{11} &= \frac{1}{2}\,(\Delta_S + \Delta_A + \Delta_R),\\
\Delta_{12} &= \frac{1}{2}\,(\Delta_S + \Delta_A - \Delta_R),\\
\Delta_{21} &= \frac{1}{2}\,(\Delta_S - \Delta_A + \Delta_R),\\
\Delta_{22} &= \frac{1}{2}\,(\Delta_S - \Delta_A - \Delta_R).
\end{aligned} \tag{29}$$

Explicitly the retarded propagator is given by

$$\begin{aligned}
\Delta_R &= \frac{1}{K^2 - m^2 + i\epsilon} - 2\pi i\,\delta(K^2 - m^2)\,n_B(k_0) + 2\pi i\,\delta(K^2 - m^2)\,[\theta(-k_0) + n_B(k_0)]\\
&= \frac{1}{K^2 - m^2 + i\epsilon} - \theta(-k_0)\,\left[\frac{1}{K^2 - m^2 + i\epsilon} - \frac{1}{K^2 - m^2 - i\epsilon}\right]\\
&= \begin{cases} (K^2 - m^2 + i\epsilon)^{-1} & k_0 > 0\\ (K^2 - m^2 - i\epsilon)^{-1} & k_0 < 0 \end{cases}\\
&= \frac{1}{K^2 - m^2 + i\,\mathrm{sgn}(k_0)\epsilon}.
\end{aligned} \tag{30}$$

It has both poles above the real axis, as shown in Fig.12. Analogously we get for the advanced propagator

$$\Delta_A = \frac{1}{K^2 - m^2 - i\,\mathrm{sgn}(k_0)\epsilon}, \tag{31}$$

which has both poles below the real axis. The symmetric propagator follows as

$$\begin{aligned}
\Delta_S &= \frac{1}{K^2 - m^2 + i\epsilon} - \frac{1}{K^2 - m^2 - i\epsilon} - 4\pi i\,\delta(K^2 - m^2)\,n_B(k_0)\\
&= -2\pi i\,\delta(K^2 - m^2)\,[1 + 2n_B(k_0)].
\end{aligned} \tag{32}$$

From these explicit expressions, we see that only the symmetric propagator contains a distribution function. This fact allows for a fast calculation of the thermal contributions of diagrams.

Self energies are related to the bare and full propagators (Δ, Δ^*) via the Dyson-Schwinger equation (see below), $\Pi = \Delta^{-1} - \Delta^{*-1}$, from which together with (26) follows

$$\Pi_{11} + \Pi_{12} + \Pi_{21} + \Pi_{22} = 0. \tag{33}$$

Analogously to the propagator we define

$$\begin{aligned} \Pi_R &= \Pi_{11} + \Pi_{12}, \\ \Pi_A &= \Pi_{11} + \Pi_{21}, \\ \Pi_S &= \Pi_{11} + \Pi_{22}, \end{aligned} \tag{34}$$

where the different sign in $\Pi_{R,A}$ is a consequence of (33).

At this point we will give two important relations for the propagators and self energies in the Keldysh representation, which we will use later on:

$$\Delta_S(K) = [1 + 2n_B(k_0)]\,\mathrm{sgn}(k_0)\,[\Delta_R(K) - \Delta_A(K)], \tag{35}$$

$$\Pi_S(K) = [1 + 2n_B(k_0)]\,\mathrm{sgn}(k_0)\,[\Pi_R(K) - \Pi_A(K)]. \tag{36}$$

The proof in the case of the bare propagator is simple (see problem #4) using explicit expressions for the different components (30) to (32) and the relation (27). However, it can be shown that (35) holds also for the full propagator in equilibrium. Out of equilibrium, on the other hand, modifications are necessary, as we will discuss in chapter 5.

Finally we will consider again the scalar tadpole as an example for the use of the Keldysh representation

$$\begin{aligned} \Pi_R &= \Pi_{11} = \frac{i}{2}\, i\,(-1)\, g^2\, 4! \int \frac{d^4K}{(2\pi)^4}\, i\,\Delta_{11}(K) \\ &= i\,12\,g^2 \int \frac{d^4K}{(2\pi)^4}\, \frac{1}{2}\,(\Delta_S + \Delta_A + \Delta_R) \\ &= 12\,g^2 \int \frac{d^4K}{(2\pi)^4}\, 2\pi\, n_B(k_0)\, \delta(K^2 - m^2), \end{aligned}$$

which agrees with (17). The last step follows from the fact that the $T = 0$-contribution vanishes after renormalization and only Δ_S contains a $T > 0$-contribution.

3 Hard Thermal Loop Resummation (HTL)

The HTL resummation technique has been developed in the late 80's and in the beginning of the 90's by Braaten and Pisarski (*Braaten, Pisarski, Nucl. Phys. B337 (1990) 569*) in order to cure serious problems of gauge theories at finite temperature using perturbation theory. For if one uses only bare propagators (and vertices), IR singularities and gauge dependent results have been encountered. A famous example is the damping rate of a plasma wave in the QGP, which turned out to be different in different gauges.

Braaten and Pisarski suggested the following solution. Instead of using bare propagators (and vertices) effective propagators, constructed by resumming certain diagrams, the so-called HTL self energies, should be adopted. In this way an improved perturbation theory has been invented.

3.1 HTL Self Energies

First we have to isolate the diagrams which should be resummed into effective propagators. The starting point is the separation of scales in the weak coupling limit. In a plasma of massless particles, we have the momentum scale T (hard) and gT (soft) assuming $g \ll 1$. HTL self energies are now given by 1-loop diagrams, where the external momenta are soft and the loop momenta hard. As an important example we will consider the photon self energy or polarization tensor in QED shown in Fig.13. At $T = 0$ it reads, using standard Feynman rules

$$\Pi^{\mu\nu}(P) = -i\, e^2 \int \frac{d^4K}{(2\pi)^4}\, \mathrm{tr}\,[\gamma^\mu\, S(Q)\, \gamma^\nu\, S(K)], \tag{37}$$

where S is the electron propagator.

For $T > 0$ we will adopt the RTF. Then we find according to Fig.14 for the retarded self energy

$$\begin{aligned}\Pi_R^{\mu\nu}(P) &= \Pi_{11}^{\mu\nu}(P) + \Pi_{12}^{\mu\nu}(P) \\ &= -i\, e^2 \int \frac{d^4K}{(2\pi)^4}\, \left\{\mathrm{tr}\,[\gamma^\mu\, S_{11}(Q)\, \gamma^\nu\, S_{11}(K)] - \mathrm{tr}\,[\gamma^\mu\, S_{21}(Q)\, \gamma^\nu\, S_{12}(K)]\right\}.\end{aligned}$$

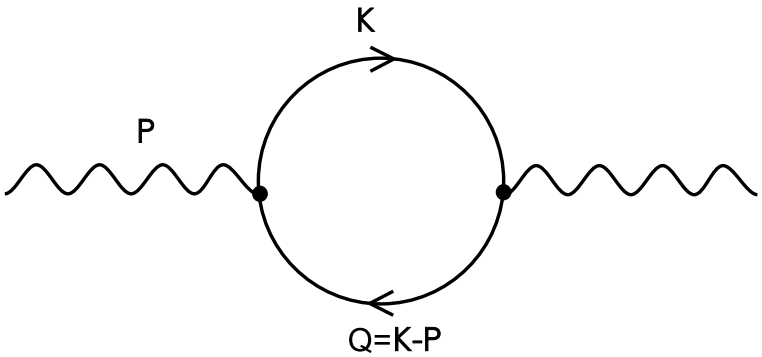

Fig.13

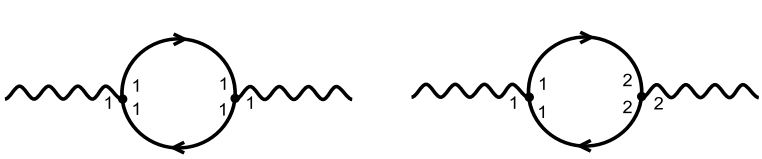

Fig.14

First we will restrict ourselves to the longitudinal component $\Pi^L_R \equiv \Pi^{00}_R$. Furthermore we neglect the bare electron mass, assuming $T \gg m_e$, which might be realized for example in a Supernova plasma ($T \simeq 10$ MeV). We write $S_{ij}(K) \equiv \not{K}\, \tilde{\Delta}_{ij}(K)$, where $\tilde{\Delta}_{ij}$ follows from Δ_{ij} by replacing n_B by $-n_F$ (compare (23) and (24)).

The trace over the γ-matrices gives

$$\begin{aligned}&\mathrm{tr}\,[\gamma^\mu \not{Q}\, \gamma^\nu \not{K}] = 4\,[Q^\mu K^\nu + K^\mu Q^\nu - g^{\mu\nu}\,(Q\cdot K)]\\ &\overset{\mu=\nu=0}{=} 4\,(2q_0k_0 - Q\cdot K) = 4(q_0k_0 + \mathbf{q}\cdot\mathbf{k}),\end{aligned}$$

from which we obtain

$$\Pi^L_R(P) = -4i\,e^2 \int \frac{d^4K}{(2\pi)^4}\,(q_0k_0 + \mathbf{q}\cdot\mathbf{k})\,\left[\tilde{\Delta}_{11}(Q)\,\tilde{\Delta}_{11}(K) - \tilde{\Delta}_{21}(Q)\,\tilde{\Delta}_{12}(K)\right].$$

The term in the square brackets of this expression within the Keldysh representation reads

$$\begin{aligned}[...] &\overset{(29)}{=} \frac{1}{4}\,[(\tilde{\Delta}_S(Q) + \tilde{\Delta}_A(Q) + \tilde{\Delta}_R(Q))\,(\tilde{\Delta}_S(K) + \tilde{\Delta}_A(K) + \tilde{\Delta}_R(K))\\ &\quad -(\tilde{\Delta}_S(Q) - \tilde{\Delta}_A(Q) + \tilde{\Delta}_R(Q))\,(\tilde{\Delta}_S(K) + \tilde{\Delta}_A(K) - \tilde{\Delta}_R(K))]\\ &= \frac{1}{2}\,[\tilde{\Delta}_S(Q)\,\tilde{\Delta}_R(K) + \tilde{\Delta}_A(Q)\,\tilde{\Delta}_S(K) + \tilde{\Delta}_A(Q)\,\tilde{\Delta}_A(K) + \tilde{\Delta}_R(Q)\,\tilde{\Delta}_R(K)].\end{aligned}$$

Note that there are no terms $\sim \tilde{\Delta}_S(Q)\,\tilde{\Delta}_S(K) \sim \delta(Q^2)\,\delta(K^2)$, which lead to singularities for $P = 0$. Also terms $\tilde{\Delta}_R(K)\,\tilde{\Delta}_A(K)$, which cannot be integrated, since there is no possibility to close the k_0-contour (pinch singularity), are absent.

The k_0-integration over $\sim \tilde{\Delta}_A(Q)\,\tilde{\Delta}_A(K)$ and $\sim \tilde{\Delta}_R(Q)\,\tilde{\Delta}_R(K)$ reduces to zero, as one can close the contour always in a half plane that does not contain a pole. Also these terms do not contribute to the $T > 0$-part of the self energy. Hence we are left with

$$\Pi^L_R(P) = -2i\,e^2 \int \frac{d^4K}{(2\pi)^4}\,(q_0k_0 + \mathbf{q}\cdot\mathbf{k})\,\left[\tilde{\Delta}_S(Q)\,\tilde{\Delta}_R(K) + \tilde{\Delta}_A(Q)\,\tilde{\Delta}_S(K)\right]$$

Replacing K by $-Q$ in the first term and using $\Delta_R(-Q) = \Delta_A(Q)$ this expression can be simplified further on,

$$\begin{aligned}\Pi^L_R(P) \quad &= \quad -4i\,e^2 \int \frac{d^4K}{(2\pi)^4}\,(q_0k_0 + \mathbf{q}\cdot\mathbf{k})\,\tilde{\Delta}_A(Q)\,\tilde{\Delta}_S(K)\\ &\overset{(31),(32)}{=} -8\pi\,e^2 \int \frac{d^4K}{(2\pi)^4}\,(q_0k_0 + \mathbf{q}\cdot\mathbf{k})\,[1 - 2n_F(k_0)]\,\delta(K^2)\,\frac{1}{Q^2 - i\mathrm{sgn}(\mathrm{q}_0)\epsilon}.\end{aligned}$$

So far this expression is exact. Now we will consider the HTL-approximation, i.e., $P \lesssim eT$ and $K \gtrsim T$. First we discuss the $T = 0$-part, corresponding to the 1 in the square brackets in the above formula. At $T = 0$ the only scale is the external momentum P. Therefore $\Pi_R^{L\,T=0} \sim e^2\,P^2$ holds. As we will see below this term is of higher order $\mathcal{O}(e^4)$ for soft momenta $P^2 \sim e^2T^2$ compared to the finite temperature part.

The $T > 0$-contribution yields after integrating over k_0

$$\begin{aligned}
\Pi_R^L(P) &= 16\pi\, e^2 \int \frac{d^4K}{(2\pi)^4}\, \frac{n_F(k_0)}{2k}\, [\delta(k_0 - k) + \delta(k_0 + k)] \\
&\quad \frac{(k_0 - p_0)k_0 + (\mathbf{k} - \mathbf{p}) \cdot \mathbf{k}}{(k_0 - p_0)^2 - (\mathbf{k} - \mathbf{p})^2 - i\mathrm{sgn}(\mathrm{k_0 - p_0})\epsilon} \\
&= \frac{e^2}{2\pi^3} \int d^3k\, \frac{n_F(k)}{k} \left[\frac{(k - p_0)k + (\mathbf{k} - \mathbf{p}) \cdot \mathbf{k}}{(k - p_0)^2 - (\mathbf{k} - \mathbf{p})^2 - i\mathrm{sgn(k - p_0)}\epsilon} \right. \\
&\quad \left. + \frac{(k + p_0)k + (\mathbf{k} - \mathbf{p}) \cdot \mathbf{k}}{(k + p_0)^2 - (\mathbf{k} - \mathbf{p})^2 - i\mathrm{sgn}(-\mathrm{k - p_0})\epsilon} \right]. \qquad (38)
\end{aligned}$$

Assuming the HTL-approximation, $|p_0|$, $p \ll k$, we will expand the integrand for small p_0/k and p/k:

$$\begin{aligned}
[...] &\simeq \frac{2k^2 - p_0k - \mathbf{p} \cdot \mathbf{k}}{-2kp_0 + 2\mathbf{k} \cdot \mathbf{p} + P^2 - i\epsilon} + \frac{2k^2 + p_0k - \mathbf{p} \cdot \mathbf{k}}{2kp_0 + 2\mathbf{k} \cdot \mathbf{p} + P^2 + i\epsilon} \\
&\simeq \frac{k}{-p_0 + p\eta - i\epsilon} + \frac{k}{p_0 + p\eta + i\epsilon} + \frac{1}{2}\, \frac{-p_0 - p\eta}{-p_0 + p\eta - i\epsilon} \\
&+ \frac{1}{2}\, \frac{p_0 - p\eta}{p_0 + p\eta + i\epsilon} - \frac{1}{2}\, \frac{P^2}{(-p_0 + p\eta - i\epsilon)^2} - \frac{1}{2}\, \frac{P^2}{(p_0 + p\eta + i\epsilon)^2} + O\left(\frac{p}{k}\right).
\end{aligned}$$

The integration over $\eta = \mathbf{p} \cdot \mathbf{k}/(pk)$ goes from -1 to 1. The sum of the first two terms is odd under $\eta \to -\eta$. Hence the first two terms vanish after integrating over η. Then we end up with the final result

$$\begin{aligned}
\Pi_R^L(P) &= \frac{e^2}{2\pi^2} \int_0^\infty dk\, k\, n_F(k) \int_{-1}^1 d\eta \left[\frac{-p_0 - p\eta}{-p_0 + p\eta - i\epsilon} + \frac{p_0 - p\eta}{p_0 + p\eta + i\epsilon} \right. \\
&- \left. \frac{P^2}{(-p_0 + p\eta - i\epsilon)^2} - \frac{P^2}{(p_0 + p\eta + i\epsilon)^2} \right] \\
&= -3\, m_\gamma^2 \left(1 - \frac{p_0}{2p} \ln \frac{p_0 + p + i\epsilon}{p_0 - p + i\epsilon} \right), \qquad (39)
\end{aligned}$$

where we introduced the effective thermal photon "mass" $m_\gamma^2 = e^2T^2/9$, coming from the k-integration over the distribution function. The lower limit of this integration is zero, although we assumed that $k \gg p$. However, the error introduced in this way is of higher order, as can be seen in the following way. Adopting a lower limit $eT \ll k^* \ll T$, we may replace $n_F(k)$ by its zero momentum limit 1/2. Then k^* is the only scale of the soft loop momentum part of the self energy. Hence it is of order

$e^2 k^{*2} \ll e^2 T^2$ and can be neglected compared to the HTL contribution. Also note that $\Pi^{T>0} \sim e^2 \gg \Pi^{T=0} \sim e^4$, justifying the neglect of the vacuum part.

Analogously we find for the transverse part of the self energy

$$\begin{aligned} \Pi_R^T(P) &\equiv \frac{1}{2}\left(\delta_{ij} - \frac{p_i p_j}{p^2}\right) \Pi_{ij}(P) \qquad (i,\, j \,\epsilon\, \{1,2,3\}) \\ &= \frac{3}{2}\, m_\gamma^2\, \frac{p_0^2}{p^2}\left[1 - \left(1 - \frac{p^2}{p_0^2}\right)\, \frac{p_0}{2p}\, \ln\frac{p_0 + p + i\epsilon}{p_0 - p + i\epsilon}\right]. \end{aligned} \tag{40}$$

At $T = 0$ there is only one independent component of the polarization tensor due to Lorentz and gauge invariance:

$$\Pi_{\mu\nu}^{T=0} = \left(g_{\mu\nu} - \frac{P_\mu P_\nu}{P^2}\right)\, \Pi(P).$$

At $T > 0$ Lorentz invariance is broken, since we have chosen the heat bath as the rest frame. But transversality, $P^\mu \Pi_{\mu\nu} = 0$, still holds as a consequence of gauge invariance. This leads to two independent components, e.g. $\Pi^{L,T}$ (see e.g. Ref.[1]).

The advanced self energy follows from the retarded one simply by the replacement

$$\Pi_A^{L,T} = \Pi_R^{L,T}(i\epsilon \to -i\epsilon). \tag{41}$$

Finally, the symmetric self energy is given by (see problem # 5)

$$\begin{aligned} \Pi_S^L(P) &= -\frac{4ie^2}{\pi p}\, \theta(p^2 - p_0^2) \int_0^\infty dk\, k^2\, n_F(k)\, [1 - n_F(k)] \\ &= -6\pi i\, m_\gamma^2\, \frac{T}{p}\, \theta(p^2 - p_0^2), \end{aligned} \tag{42}$$

$$\Pi_S^T(P) = -3\pi i\, m_\gamma^2\, \frac{T}{p}\, \left(1 - \frac{p_0^2}{p^2}\right)\, \theta(p^2 - p_0^2). \tag{43}$$

Note that it is of lower order, $\mathcal{O}(eT^2)$, than the retarded and advanced self energies for soft momenta $p \sim eT$. Furthermore it is purely imaginary.

Now a couple of remarks are in order:

1. Using the ITF one obtains the same results. In this case one has to continue analytically the discrete imaginary energy $p_0 = 2\pi i n T$ to real continuous values.

2. The HTL approximation is equivalent to the high temperature approximation, $T \gg p$, $|p_0|$, which has first been studied by *Klimov* and *Weldon* in 1982, and to the semiclassical approximation discussed already in 1960 by *Silin*.

3. In contrast to the tadpole $\Pi^{L,T}$ are momentum dependent.

4. For $p_0^2 < p^2$ the self energy has an imaginary part

$$\ln\frac{p_0 + p \pm i\epsilon}{p_0 - p \pm i\epsilon} = \ln\left|\frac{p_0 + p}{p_0 - p}\right| \mp i\pi\, \theta(p^2 - p_0^2), \tag{44}$$

describing the collisionless energy transfer from the plasma modes (see below) to the thermal particles of the plasma (Landau damping).

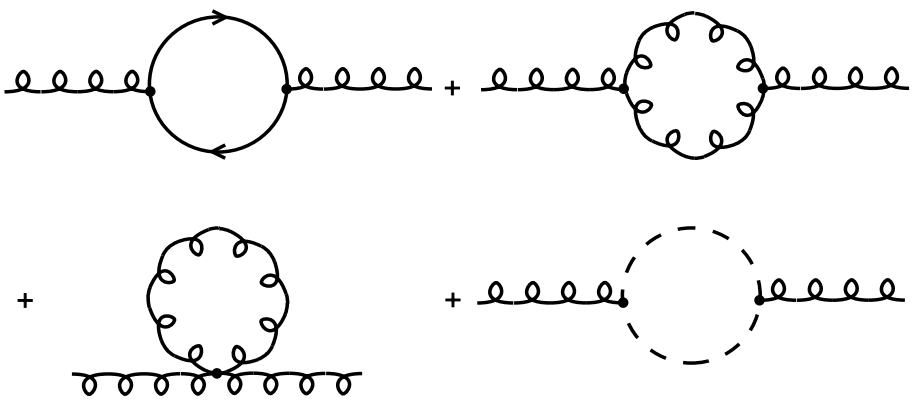

Fig.15

5. In the static limit, $p_0 \to 0$, the longitudinal self energy reduces to

$$\Pi^L_{R,A}(p_0 \to 0, p) = -3m_\gamma^2, \tag{45}$$

which leads to Debye screening of the electric interaction due to the presence of charges in the plasma. However, the transverse part reduces to

$$\Pi^T_{R,A}(p_0 \to 0, p) = 0, \tag{46}$$

i.e., there is no static magnetic screening in the plasma.

6. Considering QCD instead of QED, the gluon self energy is given by Fig.15. Surprisingly (39) to (43) still hold within the HTL approximation if we simply replace

$$m_\gamma^2 \to m_g^2 = \frac{g^2 T^2}{3} \left(1 + \frac{N_f}{6}\right), \tag{47}$$

where N_f is the number of active flavors in the QGP. Since the 1-loop QED polarization tensor is gauge invariant, the same holds for the QCD one, which has the same form.

7. The fermion self energy can also be derived within the HTL approximation (see Fig.16). Starting from the most general ansatz for massless fermions at $T > 0$,

$$\Sigma_R(P) = -a(p_0, p)\not{P} - b(p_0, p)\gamma_0 \tag{48}$$

with

$$\begin{aligned} a(p_0, p) &= \frac{1}{4p^2} \left[\mathrm{tr}(\not{P}\, \Sigma_R) - p_0\, \mathrm{tr}(\gamma_0\, \Sigma_R)\right], \\ b(p_0, p) &= \frac{1}{4p^2} \left[P^2\, \mathrm{tr}(\gamma_0\, \Sigma_R) - p_0\, \mathrm{tr}(\not{P}\, \Sigma_R)\right], \end{aligned} \tag{49}$$

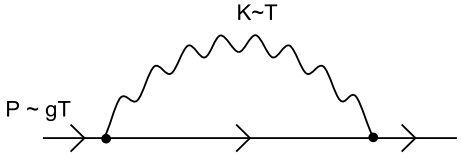

Fig.16

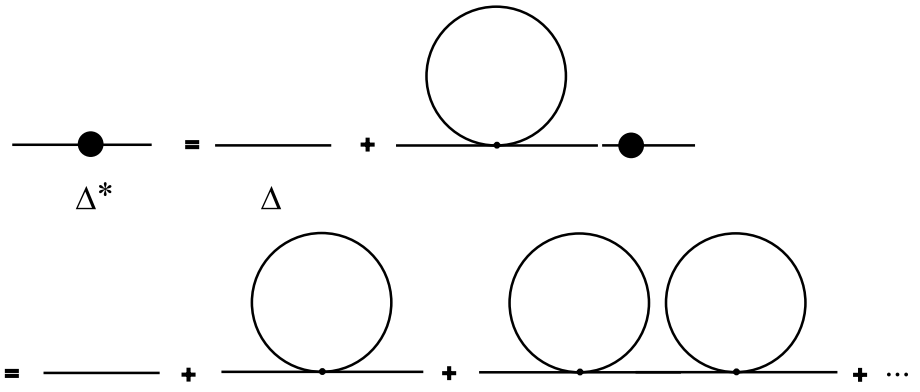

Fig.17

one finds in the HTL approximation

$$\begin{aligned} \mathrm{tr}(\not{P}\,\Sigma_R) &= 4\,m_F^2\,, \\ \mathrm{tr}(\gamma_0\,\Sigma_R) &= 2\,m_F^2\,\frac{1}{p}\,\ln\frac{p_0+p+i\epsilon}{p_0-p+i\epsilon} \end{aligned} \tag{50}$$

with the effective fermion mass $m_F^2 = e^2T^2/8$ (QED) and $m_F^2 = g^2T^2/6$ (QCD). Again one can show that the fermion self energy, (48) to (50), is gauge independent.

3.2 Effective propagators and dispersion relations

3.2.1 ϕ^4-theory

The pole of the bare propagator, $\Delta(K) = 1/(K^2 - m^2)$, describes the dispersion relation of a non-interacting, scalar particle: $K^2 - m^2 = k_0^2 - \omega_k^2 = 0$, i.e. $k_0 = \omega_k = \sqrt{k^2+m^2}$. (Here we use the notation $\Delta(K) = \Delta_R(K)$ and omit $i\epsilon$.)

We can construct an effective propagator by resumming the self energy using the Dyson-Schwinger equation as shown in Fig.17. This diagrammatic equation reads

$$\begin{aligned} i\Delta^* &= i\Delta + i\Delta(-i\Pi_1)i\Delta^* \\ \Delta^* &= \Delta + \Delta\Pi_1\Delta + \Delta\Pi_1\Delta\Pi_1\Delta + ... \\ &= \Delta\sum_{n=0}^{\infty}(\Pi_1\Delta)^n \\ &\overset{g\ll 1}{=} \Delta\frac{1}{1-\Pi_1\Delta} = \frac{1}{\Delta^{-1}-\Pi_1} = \frac{1}{K^2-m^2-\Pi_1}. \end{aligned} \tag{51}$$

The pole of the effective propagator determines the dispersion relation of an interacting collective mode with the effective mass $M = \sqrt{m^2+\Pi_1}$. (Effective masses, generated by the interaction with a medium, have been introduced in various problems in physics, e.g. the effective mass of electrons in crystals.) The dispersion relation of the collective scalar particle is simply given by the one of a massive particle, $\omega(k) = \sqrt{k^2+M^2}$ (see dashed line in Fig.20).

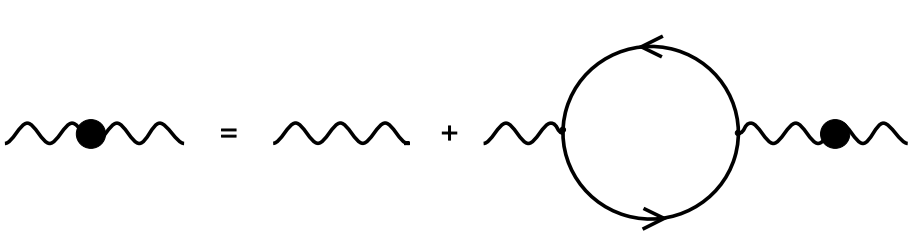

Fig.18

3.2.2 QED

In gauge theories we have to fix the gauge in order to determine the dispersion relations for a gauge boson from its propagator. At finite temperature it is convenient to choose the Coulomb gauge $\nabla \cdot \mathbf{A} = 0$. Since Lorentz invariance is broken, the choice of a non-covariant gauge is no problem. The bare propagator is then given by

$$\begin{aligned} D_{00}(K) &\equiv D_L(K) = \frac{1}{k^2}, \qquad D_{0i} = D_{i0} = 0, \\ D_{ij}(K) &\equiv \left(\delta_{ij} - \frac{k_i k_j}{k^2}\right) D_T(K), \qquad D_T(K) = \frac{1}{K^2}, \end{aligned} \tag{52}$$

where we used $D = D_{R,A}$, $\Pi = \Pi_{R,A}$. The longitudinal propagator D_L cannot be associated with a real photon but with the Coulomb potential, i.e. electric interactions. The transverse propagator D_T, on the other hand, describes 2 transverse massless photons and the magnetic interaction.

The Dyson-Schwinger equation, shown in Fig.18 gives the effective propagator

$$\begin{aligned} D_L^*(K) &= \frac{1}{k^2 - \Pi_L(K)}, \\ D_T^*(K) &= \frac{1}{K^2 - \Pi_T(K)}. \end{aligned} \tag{53}$$

(See problem # 6).

Using the HTL-approximation for $\Pi_{L,T}$ we find in the static limit: $D_L^*(k_0 = 0) = 1/(k^2 - m_D^2)$ with the Debye mass $m_D^2 = 3m_\gamma^2$, leading to screening of electric fields by the presence of charges in the plasma. For the transverse propagator we get in this limit $D_T^*(k_0 = 0) = 1/k^2$, i.e., there is no screening of static magnetic fields.

The pole of the effective propagator, ${D^*}_{L,T}(K)^{-1} = 0$, determines the HTL dispersion relations. Due to the complicated momentum dependence of the HTL self energies only numerical solutions are possible, which are shown in Fig.19. Let me make the following remarks:

1. There are two branches. The longitudinal mode ω_L is called a plasmon as in non-relativistic plasma physics. It corresponds to a collective longitudinal photon mode that is absent in vacuum.

2. For $k \to 0$ we have $\omega_L(0) = \omega_T(0) = m_\gamma$ which is called the plasma frequency.

3. For $k \to \infty$ we find $\omega_{L,T}(k \to \infty) = k$, i.e., we recover the free dispersion relation, since the self energy $\Pi \sim eT$ can be neglected for large momenta $k \gg eT$.

4. Because of $\omega_{L,T} > k$ we have $\mathrm{Im}\,\Pi_{L,T} = 0$, i.e., the HTL dispersion relations are undamped (see below).

5. The gluon dispersion relation follows from the one of a photon by simply replacing m_γ by m_g.

6. In the case of massless fermions the HTL resummed fermion propagator leads also to two branches as shown in Fig.20. The ω_+ branch corresponds to a collective electron or quark mode, whereas the ω_- branch, which has a negative ratio of helicity to chirality, does not exist in vacuum. Interestingly this so-called plasmino has a minimum at finite momentum, leading to interesting consequences for possible observables of the QGP (see below).

Finally we will discuss the symmetric HTL resummed propagator. We start from (35), which also holds for the full propagator in equilibrium,

$$D_S^{*\,L}(K) = [1 + 2n_B(k_0)]\,\mathrm{sgn}(k_0)\,[D_R^{*\,L}(K) - D_A^{*\,L}(K)].$$

Combining (41) and (44) we see that $\mathrm{Im}\,\Pi_A^L = -\mathrm{Im}\,\Pi_R^L$ holds. Therefore we have

$$D_{R,A}^{*\,L}(K) = \frac{1}{k^2 - \mathrm{Re}\,\Pi_R^L(K) \pm i\mathrm{Im}\,\Pi_R^L(K)},$$

if $\mathrm{Im}\,\Pi_R^L \neq 0$ (i.e., for $k^2 > k_0^2$ in HTL-approximation). From this we find

$$D_R^{*\,L}(K) - D_A^{*\,L}(K) = \frac{2i\mathrm{Im}\,\Pi_R^L}{(k^2 - \mathrm{Re}\,\Pi_R^L(K))^2 + (\mathrm{Im}\,\Pi_R^L(K))^2} = 2i\,\mathrm{Im}\,D_R^{*\,L}(K).$$

Now we introduce the spectral function $\rho_L = -\mathrm{Im}\,D_R^{*\,L}/\pi$. Then we can write

$$D_S^{*\,L}(K) = -2\pi i\,[1 + 2n_B(k_0)]\,\mathrm{sgn}(k_0)\,\rho_L(K). \tag{54}$$

The spectral function is of the Breit-Wigner form

$$\rho_L(K) = -\frac{1}{\pi}\,\frac{\mathrm{Im}\,\Pi_R^L}{(k^2 - \mathrm{Re}\,\Pi_R^L(K))^2 + (\mathrm{Im}\,\Pi_R^L(K))^2}$$

describing quasiparticles with finite width. Note, however, that the quasiparticle "mass" $\mathrm{Re}\,\Pi$ and "width" $\mathrm{Im}\,\Pi$ depend on momentum and energy. In the HTL approximation the self energy has an imaginary part only below the light cone ($k^2 > k_0^2$). Then the spectral function can be decomposed into a pole contribution and a cut contribution

$$\begin{aligned}
\rho_L(K) &= \rho_L^{\mathrm{pole}}(K) + \rho_L^{\mathrm{cut}}(K), \\
\rho_L^{\mathrm{pole}}(K) &= \mathrm{sgn}(k_0)\,\delta(k^2 - \mathrm{Re}\,\Pi_L^R(K)), \\
\rho_L^{\mathrm{cut}}(K) &= -\frac{1}{\pi}\,\frac{\mathrm{Im}\,\Pi_R^L(K)}{(k^2 - \mathrm{Re}\,\Pi_R^L(K))^2 + (\mathrm{Im}\,\Pi_R^L(K))^2}\,\theta(k^2 - k_0^2),
\end{aligned}$$

where one has to use the HTL results for $\mathrm{Re}\,\Pi_R^L(K)$ and $\mathrm{Im}\,\Pi_R^L(K)$.

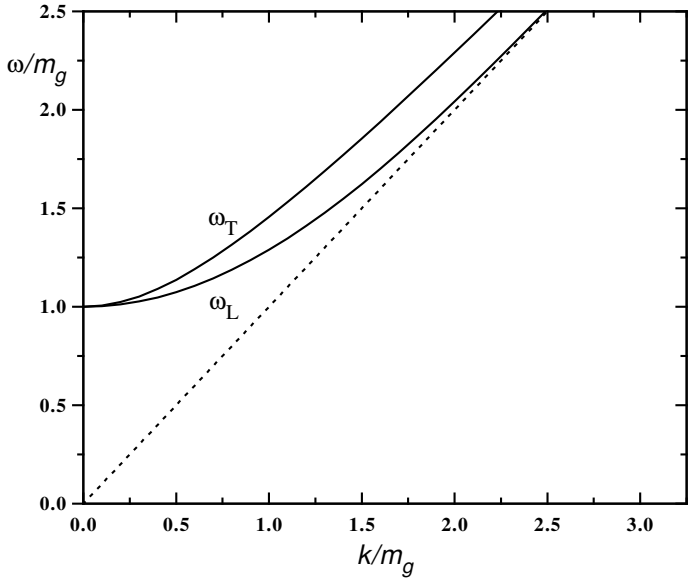
ω/m_g
2.5
2.0
1.5
1.0
0.5
0.0
ω_T
ω_L
0.0
0.5
1.0
1.5
2.0
2.5
3.0
k/m_g

Fig.19

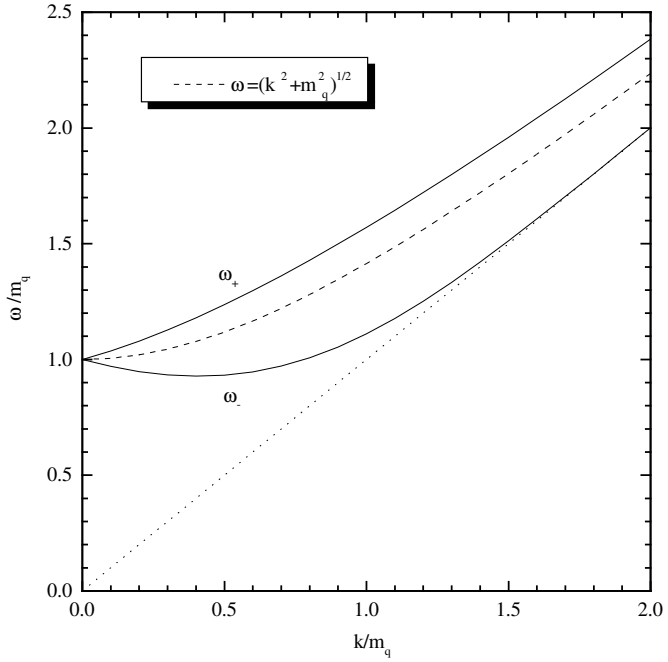
ω=(k²+m_q²)^1/2
ω/m_q
2.5
2.0
1.5
1.0
0.5
0.0
ω+
ω-
0.0
0.5
1.0
1.5
2.0
k/m_q

Fig.20

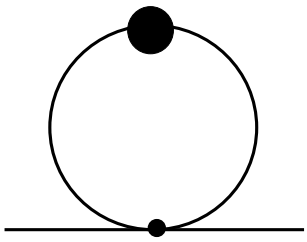

Fig.21

3.3 HTL resummation technique

As we said before, naive perturbation theory at $T > 0$ suffers from a problem, namely infrared singularities and gauge dependent results. The reason for this undesirable behaviour is that the naive perturbative expansion is incomplete at $T > 0$. Infinitely many higher order diagrams with more and more loops can contribute to lower order in the coupling constant. These diagrams can be taken into account by resummation.

3.3.1 Massless ϕ^4-theory

The lowest order tadpole shown in Fig.7 has been calculated already above, $\Pi_1 = g^2T^2 = M^2$. To next order of the scalar self energy we find a diagram as in Fig.9. This diagram exhibits a logarithmic infrared singularity because of $\Pi_2 \sim g^4 \int d^4K/K^4$. Naively we expect that the self energy can be written as $\Pi = \Pi_1 + \Pi_2 + ... = g^2T^2 + O(g^4)$.

Now we consider the tadpole diagram Π^* in Fig.21, where we have an effective propagator, $i\Delta^* = i/(K^2 - M^2)$, in the loop instead of a bare one. Since the effective propagator follows from a resummation of the bare tadpole, Π^* is given by Fig.22, i.e., it is a sum of all daisy diagrams. In order to calculate Π^* we simply have to replace the bare mass in Π_1 by the effective mass M and obtain

$$\Pi^* = 12\, g^2 \int \frac{d^3k}{(2\pi)^3}\, [1 + 2n_B(\Omega_K)], \qquad \Omega_k \equiv \sqrt{k^2 + M^2}.$$

The k-integral cannot be done analytically, but an expansion for small g is possible (see problem # 8):

$$\Pi^* = g^2T^2\, [1 - \frac{3}{\pi}\, g + O(g^2)]. \tag{55}$$

This surprising result deserves two comments:

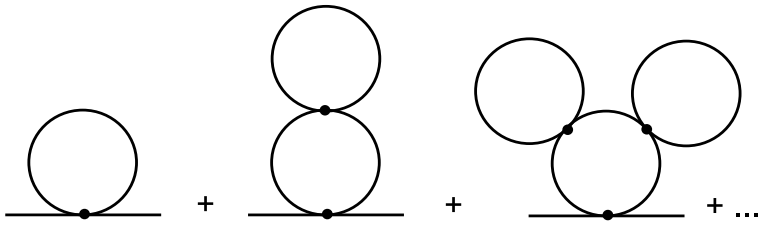

Fig.22

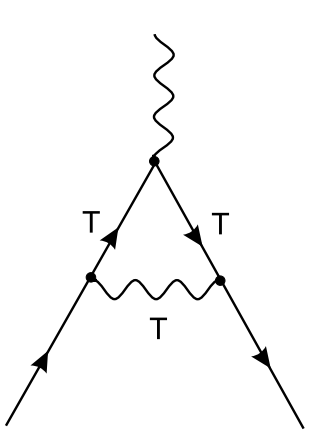

Fig.23

1. Π^* is infrared finite, although it contains (infinitely many) infrared divergent diagrams.

2. The correction to Π_1 is of order g not g^2, i.e., it is a non-perturbative correction, since it is not a power of the perturbative expansion parameter g^2.

These observations suggest the following recipe:

1. Isolate terms $\sim g^2T^2$. Here: Π_1.

2. Construct the effective propagator by resummation: Here: Δ^*.

3. Use $\Delta^*(K)$ as in perturbation theory, if k_0 *and* k are soft ($\sim gT$), because then all terms in the denominator of the effective propagator are of the same order, $\Delta^* = 1/(g^2T^2)$. If k_0 *or* k are hard ($\sim T$), however, it is sufficient to use the bare propagator, which is then of order $\Delta = 1/K^2 \sim 1/T^2$.

In Π^* we have integrated over k and k_0 from 0 to ∞. The soft momentum range is important for the correction to Π_1. Therefore it is necessary to use Δ^*.

3.3.2 Gauge theories

Here we do not want to discuss the HTL resummation technique for gauge theories in detail, but will only take over the arguments from the scalar theory. Our findings above suggest the following strategy:

1. step: Isolation of self energies $\sim g^2T^2$

These are the HTL self energies $\Pi_{L,T}$ and Σ, which we discussed already in detail. In contrast to the scalar theory there is a new aspect: due to Ward identities self energies are related to vertices, e.g.

$$ie\,[\Sigma(P_1) - \Sigma(P_2)] = (P_1 + P_2)_\mu \Gamma^\mu(P_1, P_2).$$

Therefore we have to consider also HTL vertex corrections, as shown in Fig.23, where all internal lines are hard $\sim T$.

2. step: Effective propagators and vertices

Effective propagators are constructed as above making use of the Dyson-Schwinger equations. The HTL vertex following simply by adding the HTL correction to the bare vertex. Examples are shown in Fig.24.

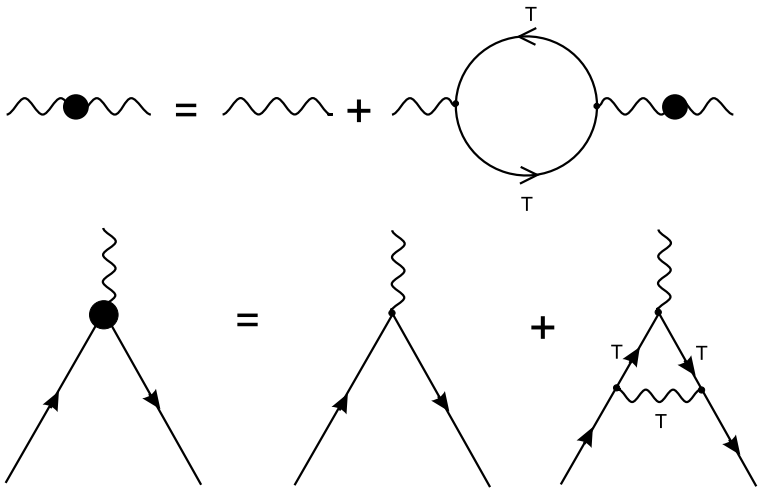

Fig.24

3. step: Effective perturbation theory

We use effective propagators and vertices if *all* legs are soft; otherwise bare propagators and vertices are sufficient. In this way, contributions of the same (or even lower) order in g are included, gauge independent results are obtained, and screening effects are included leading to an improved IR behaviour.

Summarizing, a large progress compared to naive perturbation theory has been achieved, although there are still problems, as we will see below.

4 Applications

4.1 Muon damping rate

The simplest application of the HTL resummation technique for gauge theories is the interaction or damping rate γ of a heavy fermion with mass M in a relativistic plasma, e.g. muons in an e^+-e^--plasma at $m_e \ll T \ll M_\mu$. The interaction rate is related to the mean free path by $\lambda = 1/\gamma$.

The damping or interaction rate describes the damping of a particle with the time evolution $\exp(-i\omega t)$ (plane wave). In general the frequency ω has a real and an imaginary part: $\omega = \mathrm{Re}\,\omega + i\,\mathrm{Im}\,\omega$. Defining $\gamma \equiv -\mathrm{Im}\,\omega$ we have $\exp(-i\omega t) = \exp(-i\mathrm{Re}\,\omega t)\,\exp(-\gamma t)$. As an example we consider a scalar field. Its dispersion relation is given by $\omega^2 - k^2 - \Pi(\omega, k) = 0$, from which we find

$$(\mathrm{Re}\,\omega - i\gamma)^2 - k^2 - \mathrm{Re}\,\Pi(\mathrm{Re}\,\omega - i\gamma, k) - i\mathrm{Im}\,\Pi(\mathrm{Re}\,\omega - i\gamma, k) = 0. \tag{56}$$

In the case of no overdamping, $\gamma \ll \mathrm{Re}\,\omega$, we get

$$\mathrm{Re}^2\omega - k^2 - \mathrm{Re}\,\Pi(\mathrm{Re}\,\omega, k) = 0, \tag{57}$$

from which the dispersion relation $\mathrm{Re}\,\omega = \omega(k)$ follows, and

$$-2i\,\mathrm{Re}\,\omega\,\gamma = i\,\mathrm{Im}\,\Pi(\mathrm{Re}\,\omega, k), \tag{58}$$

which leads to

$$\gamma = -\frac{1}{2\omega(k)}\,\mathrm{Im}\,\Pi(\omega(k), k). \tag{59}$$

In the case of a fermion with mass M the interaction rate is given by

$$\Gamma(E) = -\frac{1}{2E}\,[1 - n_F(E)]\,\mathrm{tr}\,[(\not{P} + M)\,\mathrm{Im}\,\Sigma_R(E, \mathbf{p})], \tag{60}$$

where $E^2 = p^2 + M^2$ and Σ_R is the retarded self energy of the massive fermion.

In naive perturbation theory the self energy to lowest order is given by Fig.25, which has no imaginary part on-shell, $\mathrm{Im}\,\Sigma_R(E, \mathbf{p}) = 0$. (A bold line denotes a massive fermion.) For according to cutting rules the imaginary part of Σ can be related to the matrix element of Fig.26, which describes the emission or absorption of a photon from a bare muon. However, this process is forbidden by energy-momentum conservation.

To next order we have to consider the 2-loop diagram of Fig.27. Using cutting rules it corresponds $\mu e^\pm \to \mu e^\pm$ scattering, which leads to an energy loss of a muon in

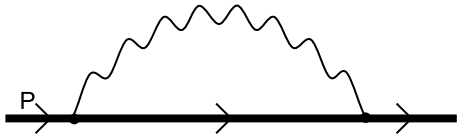

Fig.25

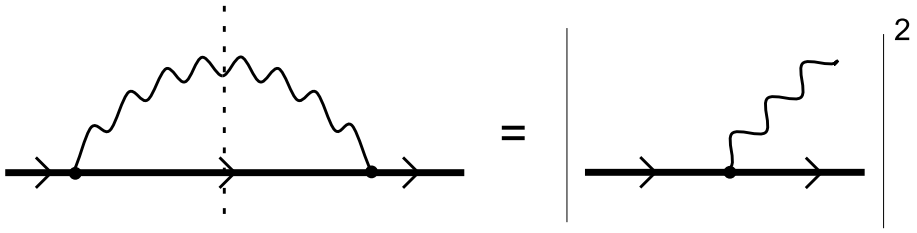

Fig.26

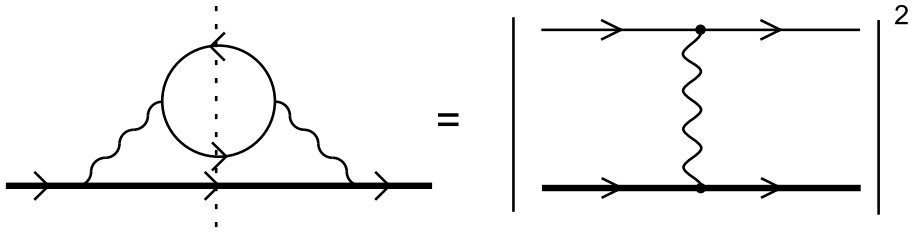

Fig.27

the e^+-e^--plasma. From naive power counting we expect $\Gamma(E) \sim \alpha^2$. However, due to the exchange of a massless photon the damping rate turns out to be quadratically IR divergent.

Therefore we have to adopt the HTL method, which leads to the diagram of Fig.28. Due to the non-vanishing imaginary part of the photon self energy contained in the HTL photon propagator of the exchanged photon this diagram has a finite imaginary part and corresponds to scattering via the exchange of a soft photon (virtual Landau damping). Note that the HTL photon self energy contains hard (thermal) electrons. Furthermore the HTL resummed photon propagator contains Debye screening. Note also that we do not need an effective muon-photon vertex or an effective muon propagator as the momenta P, P' are always hard due to the large muon mass.

Using standard Feynman rules we find at $T = 0$

$$\Sigma^*(P) = i\, e^2 \int \frac{d^4Q}{(2\pi)^4}\, D^*_{\mu\nu}(Q)\, \gamma^\mu\, S(P')\, \gamma^\nu. \tag{61}$$

At finite temperature, using the RTF, we find

$$\begin{aligned}\Sigma^*_R(P) &= \Sigma^*_{11}(P) + \Sigma^*_{12}(P) \\ &= ie^2 \int \frac{d^4Q}{(2\pi)^4}\, [D^{*\,11}_{\mu\nu}(Q)\gamma^\mu\, S^{11}(P')\, \gamma^\nu - D^{*\,12}_{\mu\nu}(Q)\gamma^\mu\, S^{12}(P')\, \gamma^\nu].\end{aligned}$$

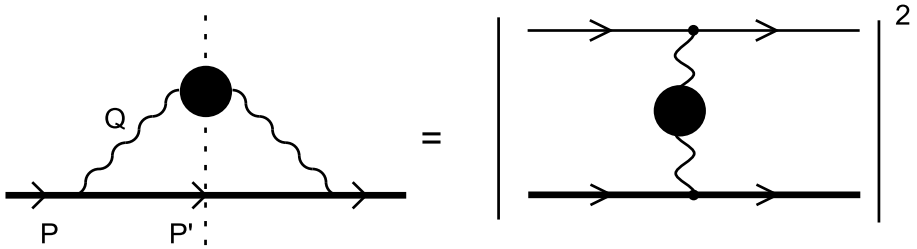

Fig.28

Defining $S(P') = (\not{P}' + M)\,\tilde{\Delta}(P')$ and using

$$D^*_{\mu\nu}\gamma^\mu\,(\not{P}' + M)\,\gamma^\nu \stackrel{(52)}{=} D^*_L\gamma^0(\not{P}' + M)\gamma^0 + D^*_T\left(\delta_{ij} - \frac{q_iq_j}{q^2}\right)\gamma^i(\not{P}' + M)\gamma^j$$

and

$$\begin{aligned}
&\mathrm{tr}\,[(\not{P} + M)\gamma^0(\not{P}' + M)\gamma^0] = 4(2p_0p'_0 - P\cdot P' + M^2)\\
&\left(\delta_{ij} - \frac{q_iq_j}{q^2}\right)\,\mathrm{tr}\,[(\not{P} + M)\gamma^i(\not{P}' + M)\gamma^j] = 8[p_0^2 - p_0q_0 - (\mathbf{p}\cdot\hat{\mathbf{q}})^2 + \mathbf{p}\cdot\mathbf{q} - M^2]
\end{aligned}$$

we find

$$\begin{aligned}
&\mathrm{tr}\,[(\not{P} + M)\,\Sigma^*_R(P)] =\\
&4ie^2\int\frac{d^4Q}{(2\pi)^4}\{\tilde{\Delta}_{11}(P')\,[D^{L\,*}_{11}(Q)\,(p_0^2 + p^2 - p_0q_0 - \mathbf{p}\cdot\mathbf{q} + M^2)\\
&+2\,D^{T\,*}_{11}(Q)\,(p_0^2 - p_0q_0 + \mathbf{p}\cdot\mathbf{q} - (\mathbf{p}\cdot\hat{\mathbf{q}})^2 - M^2)] - [(11)\to(12)]\}.
\end{aligned}$$

Using the Keldysh representation we obtain

$$\tilde{\Delta}_{11}\,D^*_{11} - \tilde{\Delta}_{12}\,D^*_{12} \stackrel{(29)}{=} \frac{1}{2}\,[\tilde{\Delta}_R\,D^*_S + \tilde{\Delta}_R\,D^*_A + \tilde{\Delta}_S\,D^*_R + \tilde{\Delta}_A\,D^*_R].$$

The leading contribution in the coupling constant e comes from $n_B(k_0 \sim eT) = 1/[\exp(|k_0|/T) - 1] \simeq T/|k_0| \sim 1/e$, which appears only in the first term. Therefore to lowest order we have

$$\begin{aligned}
&\mathrm{tr}\,[(\not{P} + M)\,\Sigma^*_R(P)] \stackrel{(54)}{=} 4\pi e^2\int\frac{d^4Q}{(2\pi)^4}\,[1 + 2n_B(q_0)]\,\mathrm{sgn}(q_0)\\
&[(p_0^2 + p^2 - p_0q_0 - \mathbf{p}\cdot\mathbf{q} + M^2)\,\rho_L(Q) + 2(p_0^2 - p_0q_0 + \mathbf{p}\cdot\mathbf{q} - (\mathbf{p}\cdot\hat{\mathbf{q}})^2 - M^2)\,\rho_T(Q)]\,\tilde{\Delta}_R(P').
\end{aligned}$$

The term $\mathrm{Im}\,\Sigma$ comes from $\mathrm{Im}\,\tilde{\Delta}_R(P') = -\pi\,\mathrm{sgn}(p'_0)\,\delta(P'^2 - M^2)$. Hence we find

$$\begin{aligned}
\Gamma(E) = &\frac{2\pi^2e^2}{E}\,[1 - n_F(E)]\int\frac{d^4Q}{(2\pi)^4}\,[1 + 2n_B(q_0)]\,\mathrm{sgn}(q_0)\\
&[(2E^2 - Eq_0 - \mathbf{p}\cdot\mathbf{q})\,\rho_L(Q) + 2(p^2 - Eq_0 + \mathbf{p}\cdot\mathbf{q} - (\mathbf{p}\cdot\hat{\mathbf{q}})^2)\,\rho_T(Q)]\\
&\mathrm{sgn}(E - q_0)\,\frac{1}{E'}\,[\delta(E - q_0 - E') + \delta(E - q_0 + E')].
\end{aligned}\tag{62}$$

Now we want to make the following approximations:

1. $E \gg T$ from which $n_F(E) \simeq 0$ follows.

2. The HTL approximation for the photon propagator: $q,\ q_0 \ll T \ll E$. This leads to

- $[1 + 2n_B(q_0)]\mathrm{sgn}(q_0) \simeq 2T/q_0$,
- $\mathrm{sgn}(E - q_0) = +$,
- the following simplification in the argument of the first δ-function:

$$E' = \sqrt{p'^2 + M^2} = \sqrt{(\mathbf{p} - \mathbf{q})^2 + M^2} \simeq \sqrt{E^2 - 2\mathbf{p}\cdot\mathbf{q}}$$

$$\simeq E\left(1-\frac{\mathbf{p}\cdot\mathbf{q}}{E^2}\right)=E-\mathbf{v}\cdot\mathbf{q},\qquad \mathbf{v}=\frac{\mathbf{p}}{E},$$

- $\delta(E-q_0+E')=0$,
- $1/E'\simeq 1/E$.

Using these approximations we find

$$\Gamma(E)=4\pi^2e^2T\int\frac{d^4Q}{(2\pi)^4}\,\frac{1}{q_0}\left[\rho_L(Q)+(v^2-(\mathbf{v}\cdot\hat{\mathbf{q}}^2))\rho_T(Q)\right]\delta(q_0-\mathbf{v}\cdot\mathbf{q}).$$

Introducing the angle η

$$\mathbf{v}\cdot\mathbf{q}=vq\eta,\qquad \eta\equiv\frac{\mathbf{p}\cdot\mathbf{q}}{pq},\qquad v=\frac{p}{E}$$

we can use the δ-function for integrating over this angle, using

$$\delta(q_0-\mathbf{v}\cdot\mathbf{q})=\frac{1}{vq}\,\delta(\eta-\frac{q_0}{vq}),$$

which gives

$$\Gamma(E)=\frac{e^2T}{2\pi v}\int_0^\infty dq\,q\int_{-vq}^{vq}\frac{dq_0}{q_0}\left[\rho_L(q_0,q)+\left(v^2-\frac{q_0^2}{q^2}\right)\rho_T(q_0,q)\right]. \tag{63}$$

Note that we integrate from 0 to ∞, although the momentum q of the photon is soft. This is possible since the intergrand drops like $1/q^3$, i.e., the integral is dominated by soft momenta regardless of the upper limit as long as it is much larger than eT. Hence the hard integration range contributes only to higher orders that have been neglected anyway.

From the intergation range of q_0 we read off that $q_0<q$. Hence only the cut contributions (Landau damping) of the spectral functions $\rho_{L,T}$ are needed.

The intergation over q in (63) can be done analytically, the one over q_0 only numerically. However, under the simplifying assumption of a non-relativistic muon, i.e., $M\gg p\Rightarrow v\ll 1\Rightarrow q_0\ll q$, we can use the quasistatic approximation for the spectral functions

$$\begin{aligned}\rho_L^{cut}(q_0,q) &= \frac{3m_\gamma^2q_0}{2q}\,|D_L^*(q_0,q)|^2\simeq\frac{3m_\gamma^2q_0}{2q}\,\frac{1}{(q^2+3m_\gamma^2)^2},\\ \rho_T^{cut}(q_0,q) &= \frac{3m_\gamma^2\omega(q^2-q_0^2)}{4q^3}\,|D_T(q_0,q)|^2\simeq\frac{3m_\gamma^2q_0q}{4}\,\frac{1}{q^6+(3\pi m_\gamma^2q_0/4)^2}.\end{aligned}$$

Here we can easily identify the Debye screening, i.e. the screening of static electric fields associated with the Debye mass $m_D^2=3m_\gamma^2$. Also we see that there is no static ($q_0=0$) magnetic screening. Using this approximation all integrations can be done exactly yielding

$$\begin{aligned}\Gamma_L(v\ll 1) &= \frac{e^2T}{4\pi},\\ \Gamma_T(v\ll 1) &= \frac{e^2T}{2\pi}\,v\int\frac{dq}{q}.\end{aligned}$$

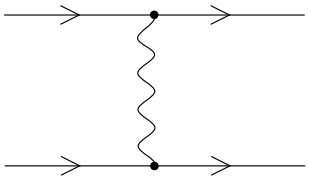

Fig.29

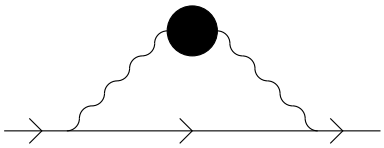

Fig.30

As expected the longitudinal part, corresponding to the exchange of an electric photon, is finite due to Debye screening, whereas the transverse part (exchange of magnetic photons) is still IR divergent. Since q is restricted to soft momenta we adopt an UV-cutoff in the above expression for Γ_T of the order $m_\gamma \sim eT$. (The UV-behaviour $1/q$ instead of $1/q^3$ in Γ_T is a consequence of the quasistatic approximation.) The IR-cutoff cannot be calculated within the HTL method. However, one can show that the damping itself provides an IR-cutoff of order e^2T. Then we obtain within the leading log approximation the final result

$$\Gamma_T(v \ll 1) = \frac{e^2 T}{2\pi}\, v\, \ln\frac{1}{e}. \tag{64}$$

Again let us make a few remarks here:

1. We have seen that in the case of the damping rate the HTL method reduces the quadratic IR divergence, found in naive perurtbation theory, to a logarithmic one.

2. Surprisingly $\Gamma \sim e^2$ and not of order e^4 as expected from naive perturbation theory. In other words, the HTL resummation leads to a lower order result (anomalous large damping) due to the strong IR sensitivty of the damping rate.

3. In the case of a heavy quark in the QGP we simply have to replace e^2 in (64) by $4g^2/3$.

4. In QCD there is an alternative IR-cutoff, namely a magnetic screening mass of the order $m_{\rm magn} = g^2T$, as suggested by non-perturbative arguments such as lattice QCD.

4.2 Other quantities

There is a number of other quantities of the QGP which have been computed using the HTL method. Here we want to give just a qualitative overview. For details we refer the reader to Refs.[2,3].

4.2.1 Energy loss, thermalization times, viscosity

The energy loss of energetic quarks and gluons ($E \gg T$) in a QGP is related to jet quenching, which might serve as a signature for the QGP formation. Energetic quarks from initial hard collisions with a large transverse momentum have to propagate through the fireball. Depending on the phase the energy loss in the fireball might be different leading to a different energy distribution of jets. The energy loss per unit length is defined as the average of the energy transfer per collision ΔE divided by

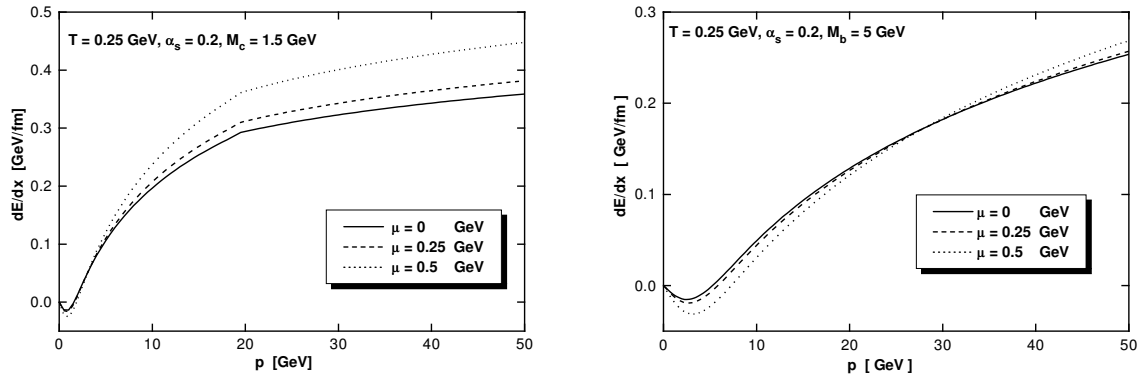

Fig.31

the mean free path $\lambda = v/\Gamma$. Hence it can be written as

$$\frac{dE}{dx} = \frac{1}{v} \int d\Gamma \Delta E$$

Due to the factor ΔE this expression is only logarithmically IR divergent in naive perturbation theory, i.e.

$$\frac{dE}{dx} \sim \int \frac{dq}{q}.$$

The energy loss can be calculated to leading order by introducing a separation scale $gT \ll q^* \ll T$ ($g \ll 1$!). For $q > q^*$ it is sufficient to use a bare gluon propagator and we find from Fig.29

$$\left(\frac{dE}{dx}\right)_{\rm hard} \sim \int_{q^*}^{E} dq... \sim \ln \frac{ET}{q^{*2}}.$$

For $q < q^*$ we need a HTL gluon propagator as in Fig.30 leading to

$$\left(\frac{dE}{dx}\right)_{\rm soft} \sim \int_{0}^{q^*} dq... \sim \ln \frac{q^{*2}}{m_g^2}.$$

Summing up the soft and the hard contributions we find

$$\frac{dE}{dx} = \left(\frac{dE}{dx}\right)_{\rm soft} + \left(\frac{dE}{dx}\right)_{\rm hard} \sim \ln \frac{ET}{m_g},$$

where the arbitrary separation scale q^* has dropped out.

The complete calculation yields the generalization of the famous Bethe-Bloch formula to the case of energetic quarks in a QGP:

$$\frac{dE}{dx} \simeq \frac{16\pi}{9}\, \alpha_s^2\, T^2\, \ln \frac{9E}{16\pi\alpha_s T},$$

shown in Fig.31 for an energetic charm and bottom quark.

Note that $dE/dx \sim \alpha_s^2$ as in naive perturbation theory, because there is only a logarithmic IR singularity in naive perturbation theory in contrast to Γ. Besides this

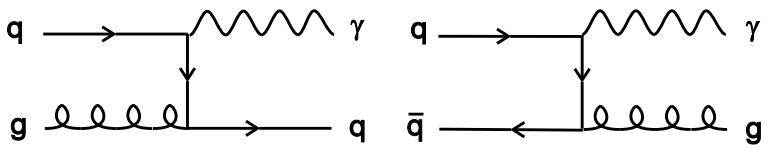

Fig.32

collisional energy loss due to elastic scattering, there is also a radiative energy loss due to gluon bremsstrahlung which turns out to be dominating in realistic situations.

The thermalization time and the viscosity of the QGP are also closely related to the damping rate and can be calculated in a similar way as the energy loss, yielding for example for the thermalization or momentum relaxation time

$$\tau^{-1} \sim \alpha_s \, T \, \ln \frac{0.2}{\alpha_s}.$$

Since the energy in the logarithm - compare with the Bethe-Bloch formula - above is now replaced by a thermal energy the extrapolation from $\alpha_s \ll 1$ to $\alpha_s > 0.2$ breaks down.

4.2.2 Photon and dilepton production

The thermal emission of real and virtual photons from the QGP has been proposed as another promising signature for the QGP formation in relativistic heavy ion collisions. Let us first consider hard real photons with an energy $E \gg T$. To lowest order naive perturbation theory these photons are produced by the diagrams of Fig.32. The photon production rate follows from the imaginary part of the two-loop photon self energy, which is related to the diagrams above again by cutting rules. In the case of a bare quark (massless) propagator we encounter a logarithmic IR singularity. Using the HTL method, we have to consider to lowest order the diagrams of Fig.33, where one HTL quark propagator appears. Due to $E \gg T$ it is sufficient to consider only one effective quark propagator.

After some more or less tedious calculations one finds for the photon production rate

$$E\frac{dR}{d^3p} = \frac{5\alpha\alpha_s}{18\pi^2} \, e^{-E/T} \left(T^2 + \frac{\mu^2}{\pi^2} \right) \ln \frac{0.13E}{\alpha_s T}, \tag{65}$$

which is shown in Fig.34.

Soft dileptons, i.e., lepton pairs from the decay of soft virtual photons ($E, p \sim gT$), can also be treated within the HTL resummation technique. Since the external photon momentum of the photon self energy is soft now, two effective quark propagators and also effective quark-photon vertices are necessary as in Fig.35. According to

Fig.33

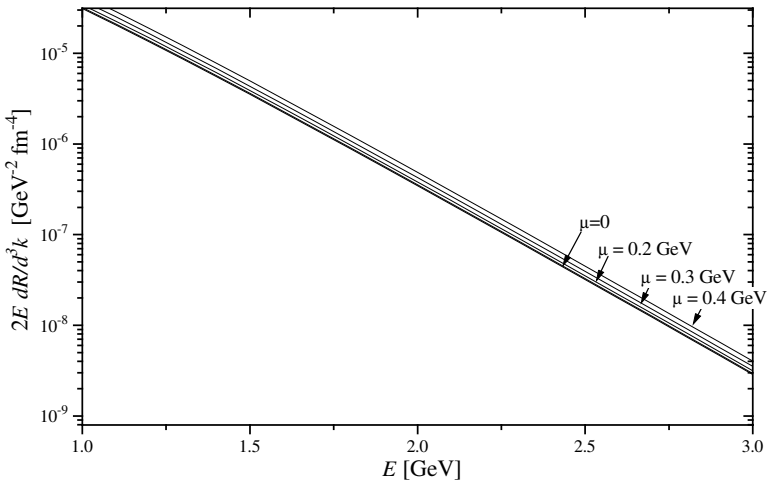

Fig.34

cutting rules this diagrams contains as physical process the annihilation of collective quarks and antiquarks. The non-trivial dispersion relation of the in-medium quarks in the HTL approximation leads to so-called Van Hove singularities in the dilepton production rate as in Fig.36, where a quantity proportional to $\mathrm{Im}\,\Pi_\mu{}^\mu$ is depicted.

Recently it has been shown that there are additional contributions to the same order from higher order diagrams (e.g. bremsstrahlung) if the invariant photon mass of is of order g^2T. Consequently the photon and ultrasoft dilepton production rates are non-perturbative and cannot be calculated to leading order even using the HTL improved perturbation theory.

Let us shortly summarize the achievements of the HTL resummation technique:

1. Using HTL resummed propagators and vertices for soft momenta, contributions of same (or even lower) order at $T > 0$ as using bare propagators and vertices can be computed.

2. At the same time medium effects (Landau damping, Debye screening) are included leading, e.g. to an improved IR-behaviour.

3. Most important it provides gauge independent results for physical quantities in contrast to naive perturbation theory.

However, there are still unsolved problems:

1. The assumption $g \ll 1$ is in contrast to realistic situations. In a QGP, expected to be produced in relativistic heavy ion collisions, we expect $\alpha_s = 4\pi/g^2 \simeq 0.2 - 0.5$, i.e. $g = 1.5 - 2.5$. The extrapolation of HTL results to such large couplings is

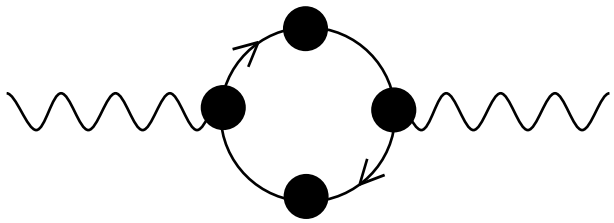

Fig.35

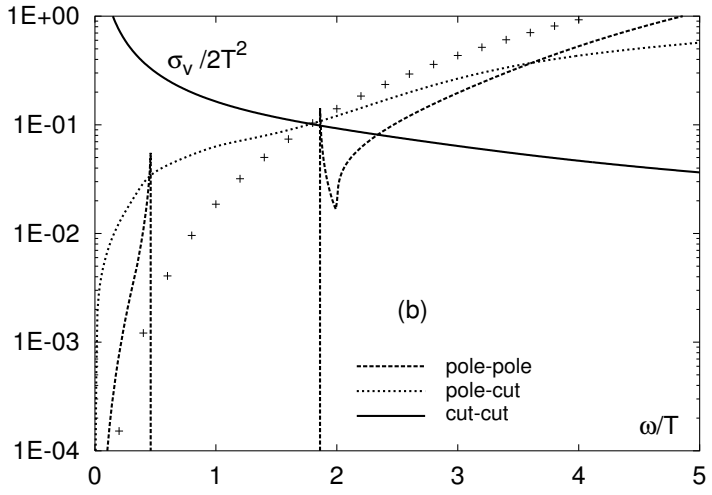

Fig.36

questionable and in the case of thermal energies $E \simeq T$ impossible (see e.g. the thermalization time).

2. There is no static magnetic screening in the HTL approximation. Hence IR singularities from the magnetic sector are not removed completely (see e.g. damping rates).

3. Some quantities cannot be calculated to leading order within HTL improved perturbation theory due to a strong IR sensitivity. For these quantities a non-perturbative resummation beyond HTL seems to be required (see e.g. the photon production rate).

4. In relativistic heavy ion collisions the QGP fireball will be out of equilibrium at least in the early stage. Therefore an extension of the HTL method to non-equilibrium situations is desirable.

5 Non-Equilibrium

If a partonic fireball is created in relativistic heavy ion collisions, it will be out of equilibrium at the beginning. Only by secondary collisions a thermal and chemical equilibrated QGP might be reached. Therefore we have to study non-equilibrium situations to describe the early stages of the fireball.

Transport models, based on the Boltzmann equation for quarks and gluons, predict a fast thermalization ($\tau_{\rm thermal} < 1$ fm/c), but a slow (or no) chemical equilibration. Hence we have to consider non-equilibrium distributions for quarks and gluons. A simple ansatz for theses distributions in thermal equilibrium, but out of chemical equilibrium is the following: $f_{F,B} = \lambda(t)\, n_{F,B}(k_0)$. Here we simply multiply the equilibrium distributions by a time-dependent factor ("fugacity"), $\lambda(t)$, which describes the deviation from chemical equilibrium. At the beginning there will be less quarks and gluons than in equilibrium, i.e. $0 < \lambda(t) < 1$.

Here we will discuss the generalization of the HTL method for quasistatic non-equilibrium situations, where the equilibration is slow compared to the processes under consideration[4]. We are not aiming at a description of the equilibration process, which is intrinsically non-perturbative. The starting point for this program is the RTF, since the ITF applies only to equilibrium. The basic idea is simply to replace the equilibrium distribution functions in (25) and (32) by non-equilibrium ones. Then it is easy to see that (39) to (41), i.e. the HTL results for the retarded and advanced polarisation tensor, still hold with

$$m_\gamma \to \tilde{m}_\gamma = \frac{4e^2}{3\pi^2} \int_0^\infty dk\, k\, f_F(k) \overset{f_F \to n_F}{\longrightarrow} \frac{e^2 T^2}{9}, \tag{66}$$

where we assumed a locally isotropic momentum distribution $f_F = f_F(k,x)$ depending on k and the space-time coordinate x. Note that in deriving (39) to (41) no assumption about the existence of a temperature has been made. The HTL method relies only on the separation of scales. Instead of the temperature T one might use the average momentum $\langle k \rangle$.

Instead of (42) (symmetric HTL polarization tensor) we get

$$\begin{aligned} \Pi_S^L(P) &= -\frac{4ie^2}{\pi p}\theta(p^2 - p_0^2) \int_0^\infty dk\, k^2\, f_F(k)\,[1 - f_F(k)] \\ &= 2iA\, \frac{\mathrm{Im}\,\Pi_R^L(P)}{p_0} \qquad \text{if } p_0^2 < p^2 \end{aligned} \tag{67}$$

with

$$A = \frac{\int_0^\infty dk\, k^2\, f_F(k)\,[1 - f_F(k)]}{\int_0^\infty dk\, k\, f_F(k)}. \tag{68}$$

In equilibrium A reduces to $2T$. Eq. (53) (retarded and advanced HTL photon propagator) holds also using the replacement $m_\gamma \to \tilde{m}_\gamma$.

[4]The ideas presented in this section are based on Ref.[4].

The most interesting quantity is the symmetric HTL propagator. We cannot use (35) here anymore as we did for deriving (54). Rather we have to go back to the Dyson-Schwinger equation for D^{*L}_S (see problem #9). It reads

$$D^{*L}_S = D^{*L}_{11} + D^{*L}_{22} = D^L_{11} + \sum_{i,j=1}^{2} D^L_{1i}\Pi^L_{ij}D^{*L}_{j1} + D^L_{22} + \sum_{i,j=1}^{2} D^L_{2i}\Pi^L_{ij}D^{*L}_{j2}.$$

Using (29) and the inverse relations of (34) we find after some manipulations

$$D^{*L}_S = D^L_S + D^L_R\Pi^L_R D^{*L}_F + D^L_S\Pi^L_A D^{*L}_A + D^L_R\Pi^L_S D^{*L}_A. \tag{69}$$

It can be shown that this equation is solved by

$$\begin{aligned} D^{*L}_S(P) &= [1+2f_B(p_0)]\,\mathrm{sgn}(p_0)\,[D^{*L}_R(P) - D^{*L}_A(P)] \\ &+\{\Pi^L_S(P) - [1+2f_B(p_0)]\,\mathrm{sgn}(p_0)\,[\Pi^L_R(P) - \Pi^L_A(P)]\}\, D^{*L}_R(P)\, D^{*L}_A(P). \end{aligned} \tag{70}$$

Here we encounter a term $\sim D^*{}_R(P)D^*{}_A(P)$. In the case of bare propagators such a term produces a pinch singularity, i.e. terms containing $\delta^2(P)$. In equilibrium, where (36) holds, the term in the curly brackets vanishes, $\{...\} = 0$. This is a consequence of detailed balance. Hence there is no pinch singularity in equilibrium.

Now we study the dangerous pinch term, i.e. the second term of (70). The following equations hold in general:

$$D^{*L}_{R,A} = (p^2 - \mathrm{Re}\,\Pi^L_R \mp i\,\mathrm{Im}\,\Pi^L_R)^{-1} \tag{71}$$

and

$$\Pi^L_R - \Pi^L_A = 2i\,\mathrm{Im}\,\Pi^L_R. \tag{72}$$

From (71) we obtain

$$D^{*L}_R\, D^{*L}_A = \frac{1}{(p^2 - \mathrm{Re}\,\Pi^L_R)^2 + (\mathrm{Im}\,\Pi^L_R)^2} = \frac{D^{*L}_R - D^{*L}_A}{2i\,\mathrm{Im}\,\Pi^L_R}, \tag{73}$$

if $\mathrm{Im}\,\Pi^L_R \neq 0$, i.e. for $p_0^2 < p^2$ within the HTL approximation. Inserting (72) and (73) in (70) yields

$$D^{*L}_S = \frac{\Pi^L_S}{2i\,\mathrm{Im}\,\Pi^L_R}\,(D^{*L}_R - D^{*L}_A). \tag{74}$$

Hence there is no pinch singularity if $\mathrm{Im}\,\Pi^L_R \neq 0$.

The physical interpretation is the following: in the case $\mathrm{Im}\,\Pi^L_R \neq 0$ the particles have a finite width (damping). Consequently the δ function is replaced by a function $\rho(P)$ of the Breit-Wigner form, i.e. a smeared δ-function. Using (67) and the definition of the spectral function (see section 3.2.2) one finds

$$D^{*L}_S(P) = -2\pi i\,\frac{A}{p_0}\,\tilde{\rho}_L(P) \tag{75}$$

with $\tilde{\rho}_L(P)$ follows from $\rho_L(P)$ using the replacement $m_\gamma \to \tilde{m}_\gamma$. In equilibrium, where we have $A \to 2T$, (75) reduces to (54) in the HTL approximation $p_0 \ll T$, for which $[1+2n_B(p_0)]\,\mathrm{sgn}(p_0) \to 2T/p_0$.

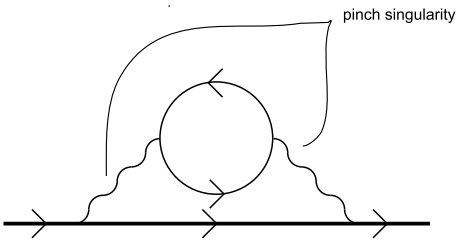

Fig.37

As an application we discuss again the damping rate of a muon in a QED plasma. The leading order contribution in naive perturbation theory suffers from a pinch singularity in non-equilibrium since there are two photon propagators of the same momentum (see Fig.37). In the HTL approximation, however, the 2-loop diagram of Fig.38 is replaced by a 1-loop diagram containing an effective gluon propagator, as in section 4.1. The photon momentum is restricted to the $Q^2 < 0$ (see (63)), where $\mathrm{Im}\,\Pi_R^L \neq 0$. Hence the HTL method also removes the pinch singularity found in naive perturbation theory. Eq. (63) reads now

$$\begin{aligned} \Gamma_{\rm neq}(E) &= \frac{e^2 A}{4\pi v} \int_0^\infty dq\, q \int_{-vq}^{vq} \frac{dq_0}{q_0} \left[\tilde{\rho}_L(q_0,q) + \left(v^2 - \frac{q_0^2}{q^2} \right) \tilde{\rho}_T(q_0,q) \right] \\ &= \frac{A}{2T}\, \Gamma_{\rm eq}(E). \end{aligned} \tag{76}$$

This result does not depend on $\tilde{m}_\gamma$ since it drops out after performing the integrations in (76).

Summarizing, we have shown, how the HTL technique can be generalized to quasistatic non-equilibrium situations. The symmetric HTL propagator contains no pinch singularity below the light cone due to Landau damping. In general, we can say that pinch singularities come from using bare propagators in perturbation theory. Resummed propagators for quasiparticles with a finite width (Breit-Wigner) do not lead to pinch singularities. In equilibrium pinch singularities are absent also for non-interacting particles due to detailed balance.

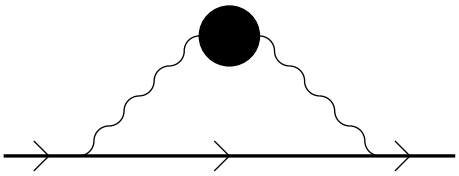

Fig.38

6 Problems

1. Calculate the particle and energy density of an ideal quark-gluon plasma containing up-, down-quarks, and gluons. Assume that the quarks are massless and that there are as many antiquarks as quarks. Use the result to estimate the critical particle and energy density for the deconfinement transition at $T_c = 170$ MeV.

   Hint: Use

   $$\zeta(n) = \frac{1}{(n-1)!}\int_0^\infty dx \frac{x^{n-1}}{e^x - 1} = \frac{1}{(1-2^{1-n})(n-1)!}\int_0^\infty dx \frac{x^{n-1}}{e^x + 1}$$

   with $\zeta(3) = 1.202$ and $\zeta(4) = \pi^4/90$.

2. Show that

   $$\begin{aligned} I \equiv T\sum_{n=-\infty}^{\infty} f(k_0 = 2\pi i n T) &= \frac{1}{2\pi i}\Big\{\int_{-i\infty}^{i\infty} dk_0 \frac{f(k_0) + f(-k_0)}{2} \\ &+ \int_{-i\infty+\epsilon}^{i\infty+\epsilon} dk_0 [f(k_0) + f(-k_0)] n_B(k_0)\Big\}, \end{aligned}$$

   if $f(k_0)$ has no poles on the imaginary axis.

   Hint: Show first

   $$I = \frac{1}{4\pi i}\oint_C dk_0 f(k_0)\coth(\beta k_0/2),$$

   where C are the contours around the poles of $\coth(\beta k_0/2)$.

3. Show that the propagator in the Keldysh representation

   $$\Delta_K = \begin{pmatrix} 0 & \Delta_A \\ \Delta_R & \Delta_S \end{pmatrix}$$

   follows from the RTF propagator

   $$\Delta = \begin{pmatrix} \Delta_{11} & \Delta_{12} \\ \Delta_{21} & \Delta_{22} \end{pmatrix}$$

   by applying an orthogonal transformation

   $$Q = \frac{1}{\sqrt{2}}\begin{pmatrix} 1 & -1 \\ 1 & 1 \end{pmatrix}.$$

4. Show that the symmetric propagator can be written as

$$\Delta_S(K) = [1 + 2n_B(k_0)]\,\mathrm{sgn}(k_0)\,[\Delta_R(K) - \Delta_A(K)].$$

5. Derive the symmetric longitudinal photon self energy in the HTL approximation and show that it fulfils the relation

$$\Pi^L_S(K) = [1 + 2n_B(k_0)]\,\mathrm{sgn}(k_0)\,[\Pi^L_R(K) - \Pi^L_A(K)].$$

   Hint: Use

$$n_F(k)[1 - n_F(k)] = -T\frac{d}{dk}n_F(k).$$

6. Show that the Dyson-Schwinger equation for the full photon propagator in Coulomb gauge leads to

$$D^*_L(K) = \frac{1}{k^2 - \Pi_L},$$
$$D^*_T(K) = \frac{1}{K^2 - \Pi_T}.$$

7. Calculate the photon dispersion relation in the HTL approximation for small $k \ll \omega$ up to order k^2.

   Hint: $\ln\frac{1+x}{1-x} = 2(x + \frac{x^3}{3} + \frac{x^5}{5} + ...)$.

8. Show that the tadpole diagram in massless ϕ^4-theory containing the effective propagator with mass $M = gT$ (sum of daisy diagrams) is given for small $g \ll 1$ by

$$\Pi^* = g^2T^2\left[1 - \frac{3}{\pi}g + O(g^2)\right].$$

   Hint: Show that the UV divergent part is of $O(g^4)$ after regularizing it by subtracting the 1-loop tadpole at $T = 0$ and introduce a separation scale $gT \ll k^* \ll T$ for evaluating the momentum integral in the small g limit.

9. Show that the Dyson-Schwinger equation for the full symmetric propagator reads

$$\Delta^*_S = \Delta_S + \Delta_R\Pi_R\Delta^*_S + \Delta_S\Pi_A\Delta^*_A + \Delta_R\Pi_S\Delta^*_A$$

   and that it is solved by the ansatz

$$\begin{aligned}\Delta_S(K) &= [1 + 2n_B(k_0)]\mathrm{sgn}(k_0)[\Delta^*_R(K) - \Delta^*_A(K)] \\ &+ \{\Pi_S(K) - [1 + 2n_B(k_0)]\mathrm{sgn}(k_0)[\Pi_R(K) - \Pi_A(K)]\}\Delta^*_R(K)\Delta^*_A(K).\end{aligned}$$

   Hint: Use $\Delta_{R,A}\Pi_{R,A}\Delta^*_{R,A} = \Delta^*_{R,A} - \Delta_{R,A}$.

Literature

1. J.I. Kapusta, *Finite-Temperature Field Theory* (Cambridge University Press, Cambridge, 1989).

2. M. Le Bellac, *Thermal Field Theory* (Cambridge University Press, Cambridge 1996).

3. M.H. Thoma, *Applications of High-Temperature Field Theory to Heavy-Ion Collisions*, in *Quark-Gluon Plasma 2*, ed. R.C. Hwa (World Scientific, Singapore, 1995) p.51 (hep-ph/9503400).

4. M.E. Carrington, H. Defu, and M.H. Thoma, *Equilibrium and Non-Equilibrium Hard Thermal Loop Resummation in the Real Time Formalism*, Eur. Phys. J. C7 (1999) 347 (hep-ph/9708363).